INSTITUTO TECNOLÓGICO Y DE ESTUDIOS SUPERIORES DE MONTERREY

MONTERREY CAMPUS

GRADUATE PROGRAM IN ENGINEERING AND INFORMATION TECHNOLOGIES

OVERLOAD PROTECTION SYSTEM USING A PCB ROGOWSKI COIL AS A CURRENT SENSOR

THESIS

PRESENTED AS A PARTIAL FULFILLMENT OF THE REQUIREMENTS FOR THE DEGREE OF:

MASTER OF SCIENCE IN ENERGY ENGINEERING

BY:

DANIEL ARGUELLES PEREZ

MONTERREY , N.L. MAY 2013

INSTITUTO TECNOLÓGICO DE ESTUDIOS SUPERIORES DE MONTERREY

SCHOOL OF ENGINEERING AND INFORMATION TECHNOLOGIES

GRADUATE PROGRAM

The members of the thesis committee hereby approve the thesis of Daniel Arguelles Pérez as a partial fulfillment of the requirements for the degree of Master of Science in Energy Engineering.

Thesis Committee:

Graciano Dieck Assad, Ph.D.
Thesis advisor

Federico Angel Viramontes Brown, Ph.D.
Synodal

Efraín Gutiérrez Villanueva, M.Sc.
Synodal

Osvaldo Miguel Micheloud Verackt, Ph.D.
Director of the Master of Science program in Energy Engineering

May 2013

Overload Protection System using a PCB Rogowski Coil as a Current Sensor

BY:

Daniel Arguelles Pérez

THESIS

Presented to the Graduate Program in Engineering And Information Technologies

This Thesis is a partial requirement for the degree of Master of Science in

Energy Engineering

INSTITUTO TECNOLÓGICO Y DE ESTUDIOS SUPERIORES DE MONTERREY

May 2013

Abstract

A very reliable overload protection system is proposed for many industrial controls of electric motor applications. The system provides a PCB Rogowski Coil (RC) high performance sensor technology, an excellent quality, a cost effective device, a saturation free sensor methodology and an easy maintenance instrumentation. The Rogowski coil (RC) and its associated electronic signal conditioning circuits implement a robust overload protection system with superior performance than the conventional current transformer (CT) technologies. A microprocessor device is used to generate the fault demand signals for three cases: overcurrent fault, current unbalance between two phases and phase current loss.

Field tests were performed for single and three phase systems to compare prototype results with simulations. They show that the device is capable to replace conventional current transformers in order to reach the output signal desired to get the correct input for the trip conditions of the overload relay system, specially for overcurrent condition. In this case the difference on trip time is higher using the SSOR than the RC sensor compared with Typical trip curve class 20 focused on current values below 180 A. The SSOR´s time differences range from 110 to 750 seconds, while the RC´s time differences range from 90 to 190 seconds. Even for critical values, the trip time difference is higher on SSOR. The SSOR works below the typical function, and the RC works pretty close of this curve. Based

on their performance, the RC sensor can be taken as a replacement of the standard CT used in the solid state overload relay to get the trip condition required.

Index   Page

List of Tables

List of Figures

Acknowledgements

Special gratitude to Dr. Graciano Dieck for his great support and guidance to develop this thesis research.

To Adrian Rendon for his great technical support.

To Dr. Federico Viramontes by all his teaching during Master Degree study and for his support to review this thesis research.

To Schneider Electric for give me the opportunity to study the Master Degree, and for your time and support to Vicente Noguez, Fabiola Gutierrez , Efrain Gutierrez , Daniel Plata, Mauricio Diaz and Gustavo Garza.

Dedication

Para mis papás Arturo y Josefina

Para Mayela y Marcelo

Chapter 1: Introduction

1.1 Justification

Technological advances in microelectronics have provided a tremendous insight to renovate and enhance instrumentation technology which seeks additional reliability, more cost effective devices, higher efficiency and portability of instruments. This research involves the study and use of current sensors based upon Rogowski coils (RC) to provide with effective means to develop overload protection systems.

An overload protection device will sample (using RCs) the operating conditions of a three phase high performance power supply and using a multi-stage electronic circuit a power supply protection system will be developed. The main goal of the project is to have higher efficiency in the measurement such that the protection system functions with better quality in providing a secure, reduced size and careful use of power resources. The main expected contributions of this project are low cost production and replacement of traditional Current Transformer (CT) sensors which have had problems of size and maintenance.

1.2 Problem description

Induction Motor is the most widely used electrical machine that allows converting electrical power to mechanical power. It has become more popular since the appearance of motor control systems. Nowadays 70% of the industrial applications uses induction machines, and they consume more than 50% of an industrialized nation’s total generating electricity. Predictive maintenance of Induction Motor drives plays an important role in the industrial community. There are different techniques for fault detection in induction machines [7].

Motor faults can be classified as electrical and mechanical faults. Among these: 1) bearing; 2) stator or armature faults; 3) eccentricity-related faults; and 4) broken rotor bar and end ring faults of induction machines are the most prevalent ones and, thus, demand special attention. Quantification of faults is as follows: 41% bearings, 37% stator faults, 12% eccentricities, and 10% broken rotor bars [11]. Overload relays are intended to protect motors, controllers, and branch-circuit conductors against excessive heating due to prolonged motor over currents up to and including locked rotor currents [25].

The important factors that must be considered to determine the appropriate overload protection are:

(a) Application Requirements.
(b) Cost.
(c) Components availability to implement the technology.
(d) Fulfillment of specifications.

Many conventional overload relays use CTs as current sampling devices. The high performance power supply, which energizes typical motor systems, uses the overload protection systems by generating three kinds of trip signals: overcurrent, phase loss and phase unbalance. The trip signal activates an actuator relay which disconnects the motor load from the power supply if the threshold level for one of the three faults appears in the system.

This Thesis investigates the substitution of conventional CTs by RC current sensor to improve the overall performance of the instrumentation device based upon the following characteristics:

1. The RCs must be developed in a Printed Circuit Boards having relatively small size (less than 5 cm in diameter).
2. The instrumentation system must provide three types of faults: overcurrent, phase loss and phase unbalance.
3. For final assembly, system must comply with this deviation for linear dimensional tolerance: +/- 0.025 [0.64 mm].
4. The size of the electronic circuitry for the three phase system should meet the actual housing dimensions of the solid state overload relay NEMA size 4 [25]. It is not part of the scope to get modified the actual housing.
5. The system must comply by testability, compatibility and reliability norms by UL 508, NEMA, IEEE, and NEC.

Other specials advantages of these RCs are: thermal stability, high linearity, high bandwidth, noise reduction due to digital integration. The most important benefit of the RC is that magnetic saturation is not present as in conventional CTs.

1.3 Objectives

The main objective of this project is to develop a device which can be used as an overload relay using RC sensor instead of the conventional CT transducer encountered in commercial solid state overload relay units. In addition, the study and understanding of Rogowski sensors serves as the leading project to introduce this transducer technology in other different products. This research is aligned to industry applications, especially for motor protection systems.

1.4 Literature Search

The RC sensor has performance characteristics that are favorable when compared to conventional CTs. They include high measurement accuracy, high precision, extremely fast response time and a wide operating current range which allows using the same device for both metering and protection. They have wide frequency range with the ability to withstand unlimited short-circuit currents, provide a design flexibility (e.g., very small to measure currents in the restricted areas where other techniques cannot be used; and flexible or rigid depending of application requirements), and involves very low production cost. In addition, RCs make protection schemes feasible in applications where conventional CTs cannot be used due to magnetic saturation, size and weight reduction. Traditional protection designs connect a number of protective and measuring equipment to conventional CTs, requiring extensive wiring. CT based systems require complex periodic testing and maintenance [6].

CTs have been traditionally used for protection and measurement applications. This is because of their ability to produce the high power output needed by electromechanical equipment. Microprocessor-based equipment makes high power output unnecessary and opens the door for ‘other measurement techniques such as RC, which have many advantages over conventional CT technology. Since the new RC is very accurate and do not saturate, protection levels can be set to lower fault current thresholds. CTs have been widely used for relay protection and current measurement. For protection applications, CT saturation is a major concern. When CTs saturate, secondary signals become distorted and may generate faulty relay operation. Using RC, magnetic saturation is not an issue due to the fact that RCs do not use iron core. Faults with dc components (asymmetrical currents) are more likely to saturate CTs, and then retain an unknown amount of flux [16].

Rogowski transducers have become an increasingly popular method of measuring current within prototyping applications and power electronics equipment due to their significant advantages compared to an equivalent CT. They possess many features which offer several advantages over iron-cored current measuring devices [18]. RC may replace conventional CTs for metering and protection. IEEE Standard C37.235-2007 [2] provides guidelines for the application of RC used for protective relaying purposes [6]. The base of this technological trend is described in patents: US5414400, US5442280 and US6313623 [26, 27, 28].

Appendix II shows a morphological analysis where sensors are applied to some electrical devices. The sensor functions are characterized as detection, protection, measurement, control and performance monitoring. The opportunity areas for potential contributions are shown in this morphological analysis. These opportunities are marked to the applications of sensors in different electrical products as well as with different functions, one of these opportunities and which seeks to develop is the application of this sensor in an overload relay having as the main function to get protection. The main objective is to deploy RC sensors with some electronics support for the purpose of getting a complete overload protection system.

1.5 Theoretical Background

RCs are transformers that operate on the same principle as conventional iron-core CTs. They were introduced in 1912 to measure magnetic fields. Today RC becomes suitable for current measurements. The RC is a uniformly wound coil on a nonmagnetic core (μ_r=1) of constant cross-sectional area formed in a closed loop. As mentioned before, Rogowski sensors have the following characteristics: non-intrusive, isolation, non-saturation at high currents, low-energy output, good linearity, high bandwidth, light weight, compact size, easy of use (can be thin and flexible), does not suffer from DC-current magnetic saturation effects, and it is relatively simple and inexpensive to manufacture [7]. The coil is placed around the conductor which current is to be measured as shown in Figure 1.1.

The main difference between RCs and CTs is that RC´s windings are wound over an air core, instead of over an iron core. As a result, RCs are linear since the air core cannot saturate. However, the mutual coupling between the primary conductor and the secondary winding in RCs is much smaller than in CTs. Therefore, RC output power is small, so they cannot drive current through low-resistance burden like CTs are able to drive [6]. The mutual inductance is independent of the current being measured. The only factor limiting linearity would be an electrical breakdown in the winding [23].

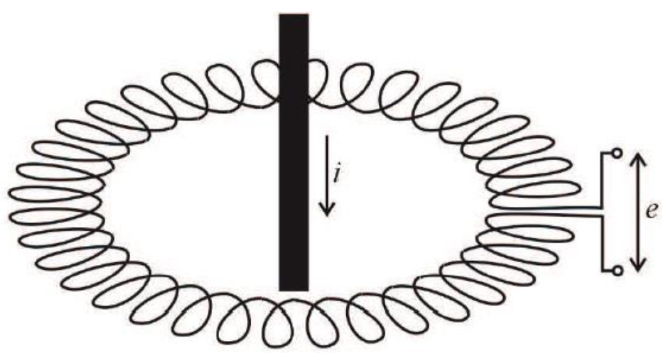

Figure 1.1 Principle of Rogowski Coil design [19].

Some minimum characterization criteria must be met when this sensor is designed, as the RC output signal should be independent of the primary conductor position inside the coil loop and the impact of nearby conductors that carry high currents on the RC output signal should be minimal. For an ideal RC, measurement accuracy depends upon the conductor location inside the coil loop [20].

According Faraday's law, a time varying voltage (e) induced by a magnetic field is expressed as follows:

$$e = -\frac{d\phi}{dt} \tag{1.1}$$

Where ϕ is the magnetic flux in Wb crossing through a closed surface. The closed surface is bounded by a conductive wire wounded n times, equation 1.1 changes to:

$$e = -n\frac{d\phi}{dt} \tag{1.2}$$

Equation 1.2 is used to calculate the output voltage from a Rogowski coil.

Amperes's law states that the line integral of the magnetic field intensity vector $\overline{H}$ over any closed path equals to the current I crossing the path. This can be expressed as follows:

Where I is the current flowing given in Amperes (A), $\overline{H}$ is the magnetic field intensity vector given in A/m, and $\overline{dl}$ is the differential length vector in meters [19].

$$\oint \overline{H} \cdot \overline{dl} = I \tag{1.3}$$

The magnetic flux density vector, $\overline{B}$ given in Wb/m^2, can be evaluated as follows:

$$\overline{B} = \mu_0 \overline{H} \tag{1.4}$$

Where μ_0 is the free space permeability having a value of $4\pi \times 10^{-7}$ H/m. In terms of current and radial distance, ρ, the magnetic flux density vector is expressed as:

$$\overline{B} = \frac{\mu_0 I}{2\pi\rho} \hat{a}_\phi \tag{1.5}$$

Where $\hat{a}_\phi$ is the unity vector in the angular direction ϕ (considering cylindrical coordinates). The magnetic flux, ϕ given in Wb, is obtained from a surface integral

$$\phi = \int_s \overline{B} \cdot \overline{ds} \tag{1.6}$$

Where $\overline{ds}$ is the surface vector passing the flux density vector $\overline{B}$. The flux is evaluated as follows:

$$\phi = \frac{\mu_0 I h}{2\pi} \ln\left(\frac{b}{a}\right) \tag{1.7}$$

Where h is the length of the coil, (thickness of the board), a is the inner radius and b is the outer radius, all in meters, as shown in figure 1.2. [19]

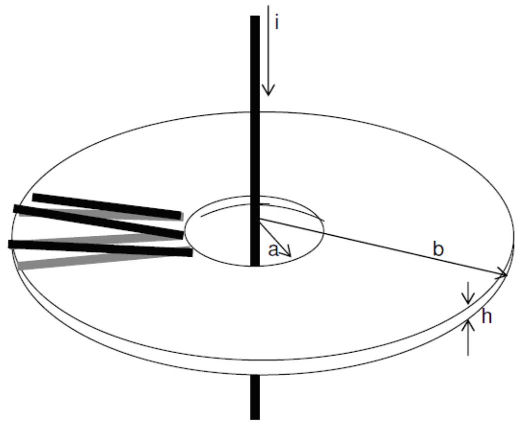

Figure 1.2 Sensor parameters a , b and h [19].

RCs generate a linear response and the impact from the nearby electromagnetic fields is minimal. To minimize the influence of neighboring conductor the turns should be uniformly distributed over the 360° of the disc formed by the single printed board sensor. The quality artwork geometry is a very important part of the RC construction and it greatly affects the sensitivity, accuracy and reliability of the sensor [18].

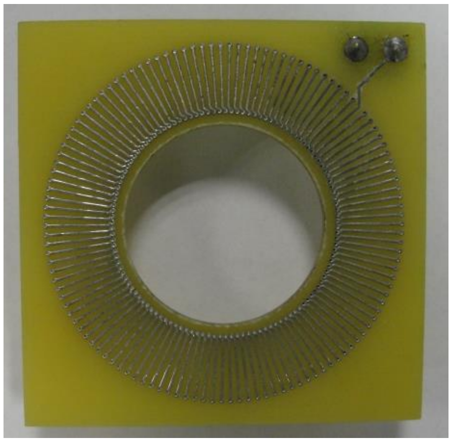

Figure 1.3 RC´s Printed Circuit Board.

To increase the accuracy of the measurement, the artwork geometry should be kept uniform along the length of the coil. Decreasing the size of the wire allows more turns per unit length, but small gauge wire is fragile and reduces the robustness of the coil. Increasing the average turns by means of additional winding layers, produces greater output but results in increased overall diameter which may limit the possible locations where the sensor can be used. The more accurately the coil is made, the better it will perform [23]. The RC output voltage is proportional to the rate of change of the measured current. RC windings are printed on the same printed circuit board (PCB). See figure 1.3.

Typical RC´s PCBs have the following characteristics: metering accuracy; measurement range from 1 A. to over 100 kA; frequency response linear up to 700 kHz, unlimited short-circuit withstand, can be installed around bushings or cables, avoiding the need for high insulation. RC can be connected in series to increase output signal [4].

Due to modest output signal levels**,** RCs should be shielded to prevent capacitive coupling to the high voltage primary conductors, and minimize influence of high frequency electromagnetic fields. RC secondary wiring will most often be placed in the vicinity of primary high voltage apparatus and multiple current carrying conductors. To minimize the impact from external electromagnetic fields, it is necessary to use shielded cables [4].

Electronic signal processing circuitry which may be placed in the immediate vicinity of the RC, and used to amplify or convert low level signals is a key factor to get transmission and measurement. Signal is forwarded in digital or analog form to other devices requiring the information.

RC may replace conventional CTs in many metering, control and protection applications. As mentioned earlier, RC can provide superior differential protection of large motors and generators since they are linear (do not saturate), reject external electromagnetic fields, and they are accurate. The RC physical dimensions and weight are much smaller than of conventional CTs, while providing simpler and more reliable protection [4]. RCs have been applied at all voltage levels (low, medium, and high voltage). However, unlike CTs that produce secondary current proportional to the primary current, RC produce output voltage that is a scaled time derivative di(t)/dt of the primary current [6].

Conventional iron-core CTs are typically designed with rated secondary currents of 1 Amp or 5 Amps, to drive low impedance burden of several ohms. ANSI/IEEE Standard C57.13™-2008 specifies CT´s accuracy class for steady state and symmetrical fault conditions. Accuracy class of the CT ratio error is specified to be ±10% or better for fault currents up to 20 times the CT rated current and up to the standard burden (maximum ohm value of burden that can be connected to the CT secondary). CTs are designed to meet this requirement. But, if a symmetric fault current exceeds 20 times the CT rated current or if the fault current is smaller but contains DC offset (asymmetric current), the CT will saturate. The secondary current will be distorted and the current RMS value reduced. CT's require heavy gauge secondary wires for interconnection to relays and other metering and control equipment. The wire resistance adds to the CT burden and negatively impacts the CT transient response and may cause CT saturation at high fault currents [6].

Voltages can be generated when the CT secondary circuit is opened while load current is flowing. The coil output signal of the RC signal is a minimal voltage from the safety aspect, and this voltage does not increase when the secondary circuit is open [6].

The cross-sectional shape upon which the coil is formed is generally either circular or rectangular. Rigid RCs have higher accuracy than flexible RCs and may be designed using PCBs as window (non-split core) type or split-core type. RC´s PCB can be designed using one or two printed circuit boards to imprint windings [6].

An electrostatic shield is required to condition the RC. Large dv/dt disturbances in close proximity to the coil produce measurement interference due to capacitive coupling. A shield eliminates this coupling. However, RCs are not normally fitted with an electrostatic shield since the resulting increase in coil capacitance reduces the high frequency bandwidth [8]. Therefore, a good recommendation is to fit an electrostatic shield around the RC when a measurement is carried out in close proximity of a large source of dV/dt external to the measurement. The shield reduces the effect of measurement interference due stray capacitance between the source of dV/dt and the transducer. The shield increases the capacitance of the RC which limits the high frequency response of the Rogowski sensor [8].

RCs may be calibrated at relatively low currents, and used with confidence at very high currents. However, the lowest level of current that can be measured is limited by the sensitivity of the voltage measuring instrument and system noise. RCs can measure currents with extremely fast rise time [9]. The RC is designed to give a high degree of rejection to external magnetic fields, for example nearby conductors. But they act sensitively by a very small amount of magnetic fields in internal magnetic fields. Signals from the sensor have a high signal-to-noise ratio (SNR) at these values, allowing the use of simple amplification and filtering techniques and resulting in AC measurement systems with better linearity, versatility, and cost compared to conventional instruments. For an ideal RC, measurement accuracy is independent of conductor location inside the coil loop [14]. When RCs were introduced, they could not be used for current measurements, since coil output voltage and power were not sufficient to drive measuring equipment. With today’s microprocessor-based protection and measurement equipment, RCs are more suitable for such applications. CTs have been traditionally used for protection and measurement applications, in part because of their ability to produce the high power output needed by electromechanical equipment. Microprocessor based equipment makes high power output unnecessary and opens the door for other measurement techniques such as RCs, which have many advantages over conventional CTs [15].

RC´s output voltage signals can be managed or conditioned by an electronic circuit. Once this conditioning is performed, a demand signal for the actuator is generated to execute the relay trip function. In the signal conditioning stage, the offset level and noise rejection greatly depends on the operational amplifier (op-amp) characteristics. In addition, the circuit needs to amplify the signal as the RC terminal voltage is very small, especially at low frequency measurements. An operational amplifier, which has a suitable combination of precision, low noise and low offset with a high gain bandwidth product and high slew rate, is used for electronic stages to normalize the signal [18].

A high performance RC has less sensitivity to the relative position of the conductor passing through the coil. It also needs to be insensitive to other current carrying conductors outside the coil [18]. The self-capacitance and self-inductance of the coil may cause a resonance. The self-resonant frequency of a coil depends on its size, on the winding details. The resonant frequency is also affected by whether or not the coil is fitted with an electrostatic screen, and by the length of the output cable between the coil and the integrator, since both of these introduce additional capacitance [23].

Some other applications of RCs are:

1. Differential protection.

2. Fault detection in induction motors. Here the RC transducer is used for fault detection and for data acquisition system in electrical machines.

3. Protection schemes including arc furnace transformers.

4. Protection systems in measurement of low frequency slip currents on wound rotor induction motors [16].

5. Applications to the measure pre-arc and post-arc currents in laboratories during interruption of short circuit current in circuit breakers [17].

6. Sudden short-circuit testing.

7. Monitoring weld quality.

8. Electromagnetic launchers.

9. On-line insulation discharge monitoring.

1.6 Thesis Organization

This thesis is organized as follows:

a. Chapter 1 describes the introduction, justification, problem description and state of the art regarding overload relay types.
b. Chapter 2 provides an overview of current sensors types and the proposed RCs as a replacement for the conventional CTs used in solid state overload relay protection systems.
c. Chapter 3 analyzes the electronic instrumentation that integrates the signal conditioning to normalize the signals coming from the RC transducers. This includes all stages to get the output signal until a digital code is generated in response to a contingency.

d. Chapter 4 describes the prototypes developed, including simulations, tests and comparative results.
e. Chapter 5 includes the conclusions, and
f. Chapter 6 provides the future directions of this research work.

Chapter 2: Overload Relays

2.1 Background

Chapter 1 illustrated that the induction motor is the most widely used electrical machine that allows converting electrical power to mechanical power. The primary objective of overload protection is to protect the motor, controller and the motor branch circuit conductors against excessive heating due to motor overloads and failure to start. If such a condition is allowed to persist for a sufficient length of time, dangerous overheating and damage may result. Under these circumstances, a properly functioning overload relay automatically causes the motor to be de-energized.

Overload relays are employed on a motor control to limit the amount of current drawn. The overload relay does not provide short circuit protection. This is the function of over current protective equipment like fuses and circuit breakers, generally located in the disconnecting switch enclosure. The overload relay is the heart of motor protection. It has inverse-trip-time characteristics, permitting it to hold in during the accelerating period (when inrush current is drawn), yet providing protection on small overloads above the full-load current when the motor is running. Overload relays are renewable and can withstand repeated trip and reset cycles without need of replacement. Overload relays cannot, however, take the place of over current protection equipment. Important benefits of the overload relay are to prevent the expense of replacing or rewinding a burned out motor, and thus prolong motor life. For NEMA or IEC products, overload relay response to stress according to these curves. These curves, shown in Figure 2.1, are defined by the required protection class.

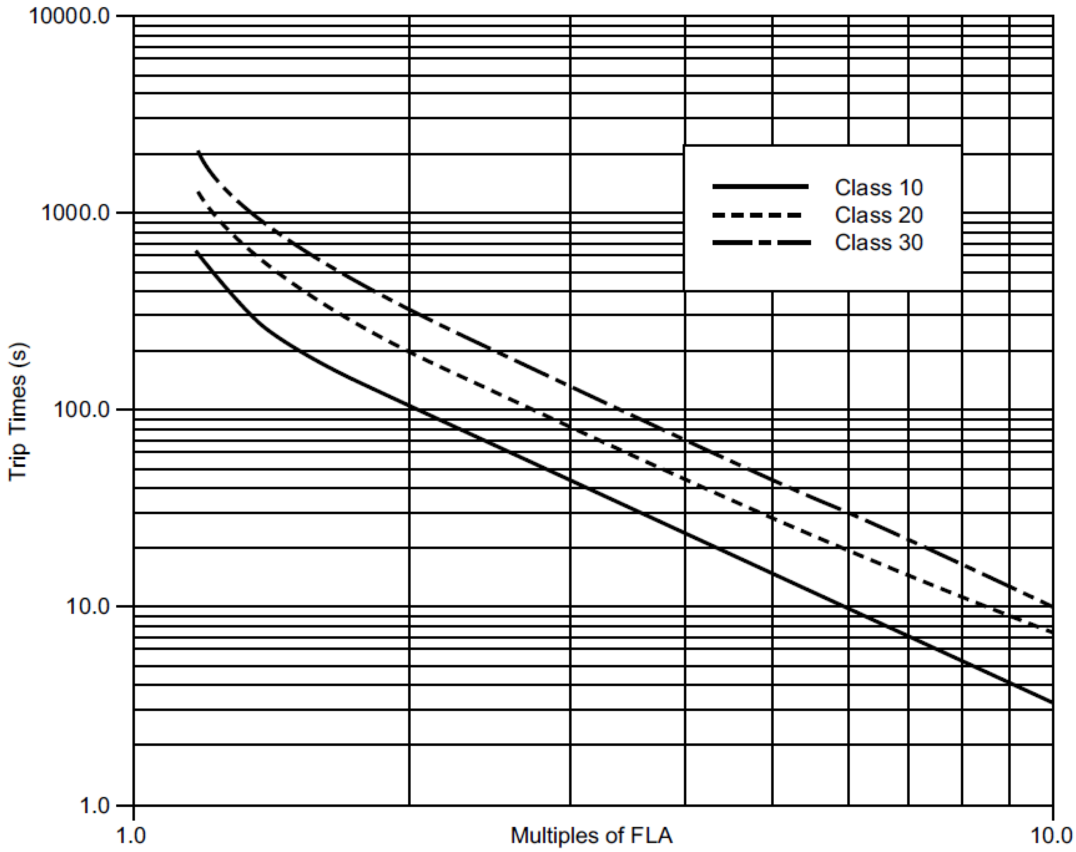

Figure 2.1 Typical curves for Trip versus current. Class 10, 20 and 30 mean that the device must respond in 10, 20 and 30 seconds or less, respectively [25].

The time to trip depends on current magnitude and length of time since last trip. Overload trip time is inversely related to current magnitude, as shown in figure 2.1. The overload relay is designed to NEMA standards for a 1.15 service factor motor. Since this is a Trip Class 20 relay, the relay trips in less than 20-seconds at currents that are 600% or more of the dial setting [25]. Overload relays in general can be classified as being thermal, bimetallic and electronic. Further details about this classification are described in section 2.2

Overload protection is intended to deal with currents ranging from motor full load current to locked rotor current (10 x full load current). Short circuit or ground fault currents can reach values much higher than 10 x full load current. Overload protection are required in each phase of a three phase circuit.

Motor terminals T1, T2, and T3 are connected to overload relay. Overload relay is connected between main contactor and motor. When an overload signal occurs, the normally closed contact (95-96) changes as an open contact, this contact is wired in series with the motor contactor coil as part of the control circuit, thus with this contact open the motor contactor coil is de energized and the contactor contacts are open, having the power circuit de energized. Figure 2.2 shows a typical control and power circuit used in motor control systems.

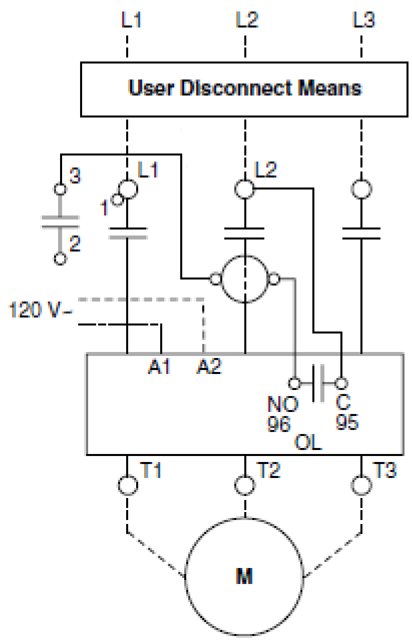

Figure 2.2 Control and power schematic diagram for overload motor control [25].

The actual solid state overload relay has an actuator located into the relay unit, when an overload signal occurs, this actuator is energized and their normally closed contact changes to open. Having the same operation as was mentioned before. Figure 2.3 shows the typical structure of the solid state overload relay system. The motor disconnect which can be a circuit breaker or a disconnect switch device in addition with the motor branch circuit protection. Figure 2.4 illustrates how both, the motor controller and the motor overload protection are enclosed into a single unit.

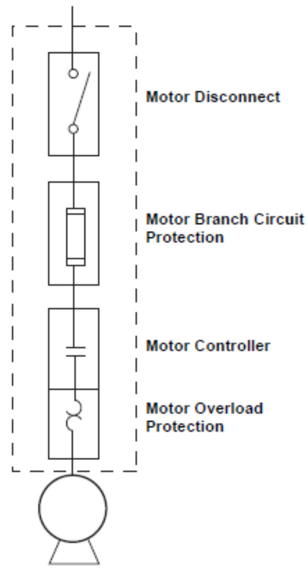

Figure 2.3 Typical structure of the solid state overload relay system [25].

Figure 2.4 Enclosed motor control system. Courtesy: Schneider Electric.

2.2 Overload Relay Systems

Overload relay systems includes a wide variety of configurations seeking robust and reliable solutions in motor protection. The representative configurations are:

a. Melting alloy
b. Non compensated bimetallic
c. Ambient temperature compensated bimetallic
d. Solid state overload relays

The following subsections describe briefly those configurations

2.2.1 Melting Alloy

The motor current passes through a winding heat under overload conditions, the heat causes a special welding fusion allowing the ratchet wheel to turn freely thus opening the contacts of the control circuit, thus having the function of shooting or trip. Once triggered, this thermal overload relay not reset until it has cooled down, automatically allowing the motor to cool before to be restarted. Figure 2.5 shows a melting alloy thermal unit with their internal elements.

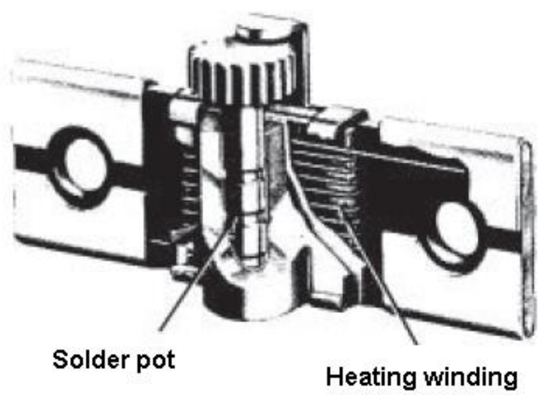

Figure 2.5: Melting alloy thermal unit [25].

2.2.2 Non compensated bimetallic

Figure 2.6 shows a bimetallic thermal relays which uses a "U" shaped bimetal strip associated with a coil. When an overload occurs, the heat will cause the bimetal to be deformed and so operate a contact in the control circuit. Thermal overload relay sense motor current by converting this current to heat in a resistance element. The heat generated is used to open a normally closed contact in series with a starter coil causing the motor to be disconnected from the line [25].

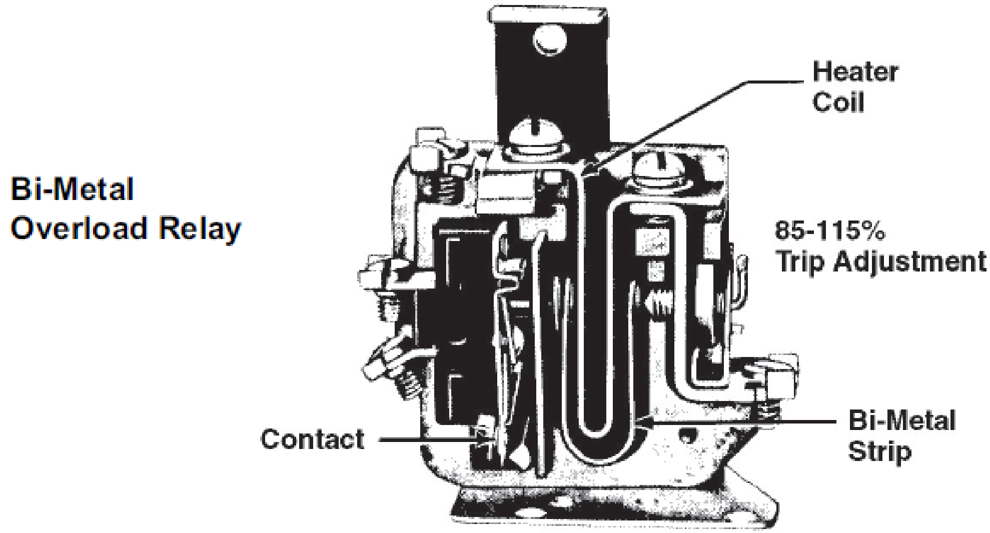

Figure 2.6 Bi-Metal overload relay [25].

2.2.3 Ambient temperature compensated bimetallic

Thermal overload relay used when the engine is operating at a constant ambient temperature and the motor controller is located separately in an environment with variable temperature. There is an independent element to the heat that compensates for this change of temperature on the controller. His trip point is not affected by temperature, and their performance is consistent to the current value. Its appearance is very similar to figure 2.6.

2.2.4 Solid state overload relay

These devices do not require thermal unit, and when they operate within their temperature range do not require compensation. Only the motor current level affects the tripping of the relay and they have phase loss protection [25]. Solid state relay also provides protection against unbalance, where the relay will trip if the current in one of the phases is 25% higher than the average of the three phases. Phase unbalances are typically caused by an unbalanced up-stream single phase load that can disturb phase voltages. Such a condition can similarly lead to excessive rotor currents and motor damage.

The most important feature offered by this electronic solid state overload relay is phase loss protection. While a phase loss causes a significant current increase in the remaining phases of the motor circuit, there is a major increase in rotor current that can cause motor damage. Figure 2.7 shows a Schneider Electric solid state over load relay with line and load terminals to get connected contactor and motor. On the cover there is a dial setting to adjust the full load amperes according with the motor application used. Figure 2.8 shows the dial setting.

2.3 Fault conditions

An electronic circuit in the overload relay detects a phase unbalance and initiates a trip when any phase current drops 25% below or rises 25% above the average of the three phase currents. The phase loss circuitry initiates a trip within 3 seconds if one of the three phase currents is not present or unbalance condition occurs. Typical overload condition operates following the trip time versus current curve [25].

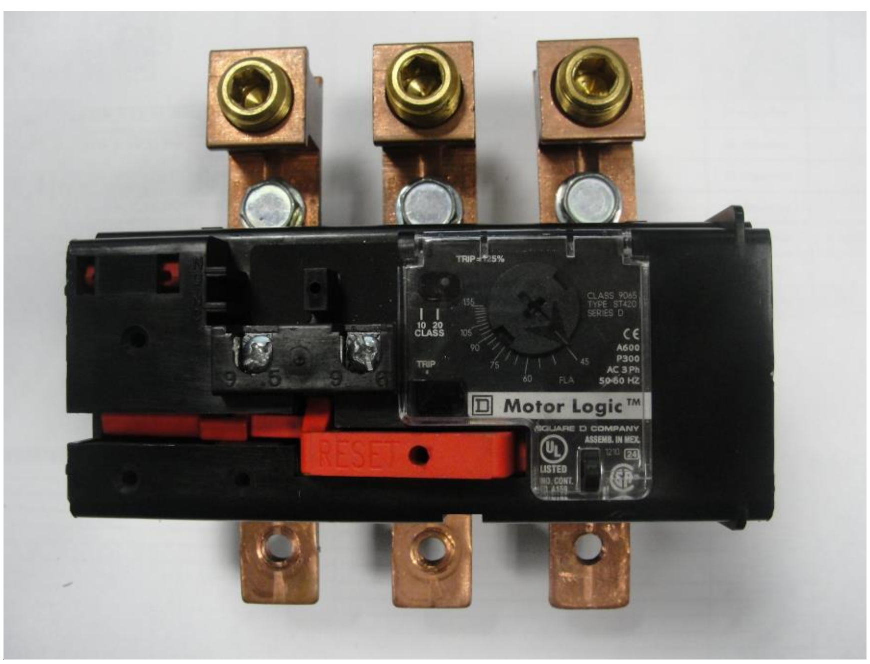

Figure 2.7: Solid state overload relay unit size 4. Courtesy: Schneider Electric.

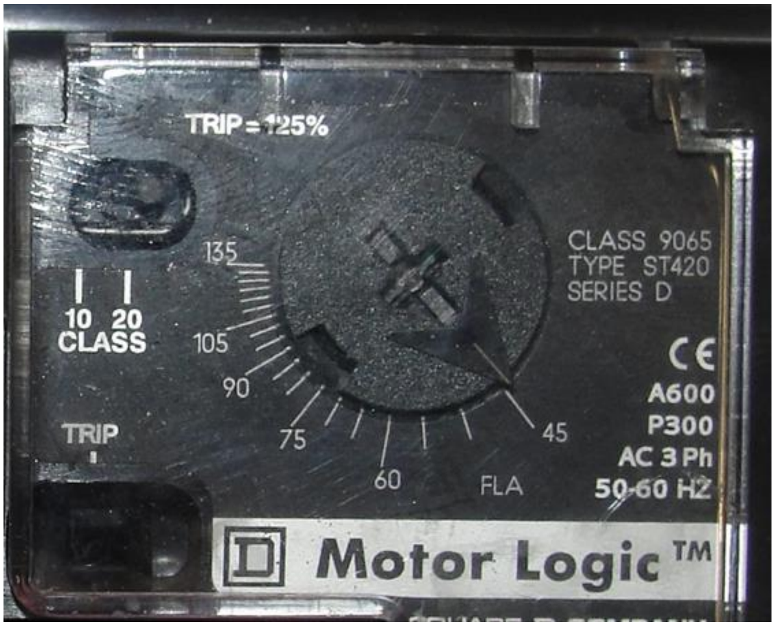

Figure 2.8 Solid state overload relay trip adjustment 45 to 135 A. Courtesy: Schneider Electric.

2.4 Current Sensors Comparison

Different current sensing methods can be used to obtain a signal proportional to current: shunt techniques, Hall Effect Sensors, CT and also the RC [3]. CTs have been employed for current sensing in fault detection of electrical machines. This solution provides galvanic isolation and allows high bandwidth measurements but the CT must be designed so that it does not saturate while carrying the DC component of the primary current, which increases its size and cost. Table 2.1 shows a comparison of different methods for measuring current. The importance of each characteristic will depend on the specifications and the purpose of the required application. The table illustrates that the RCs offer major advantages over all the characteristics that include: isolation, weight, DC and low frequency responses, fast current changes, output signal, installation and cost.

Table 2.1: Comparison of different methods for measuring current [23].

Characteristic	Coaxial shunt	Current transformer	Hall effect device	Rogowski coil
Isolation	Worst	Best	Best	Best
Weight	Worst	Regular	Regular	Best
DC response	Best	Worst	Best	Best
Low frequency response	Best	Regular	Best	Best
Fast current change	Best	Regular	Regular	Best
Output	VOLTAGE	CURRENT	VOLTAGE	VOLTAGE
Ease of installation	Worst	Regular	Regular	Best
Cost	Worst	Regular	Regular	Best

2.5 Proposed sensor

RC was based on a solid state overload relay NEMA size 4, with a current range from 45 to 135 A, and taking as reference a class 20 current-time curve. Based upon space requirements, sensor location, and conductor size, the sensor prototype was built on a PCB (2 X 2 X .062 inch) as shown in figure 2.9.

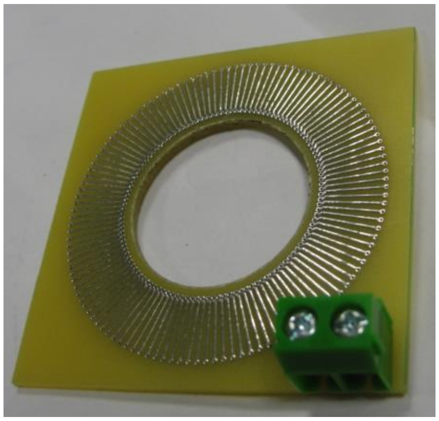

Figure 2.9 Proposed PCB sensor.

Figure 2.10 shows how the proposed sensor was designed, these parameters were used to get defined the specific size and sensor ratings h is defined as the length of the coil, a is the inner radius and b is the outer radius , all in meters and n is the number of turns which is defined as follows:

$$n = \frac{2\pi a}{w + s} \tag{2.1}$$

The relations of turns and size depend upon the PCB fabrication process and w,s are the track width, and the distance of spacing between tracks, respectively [19].

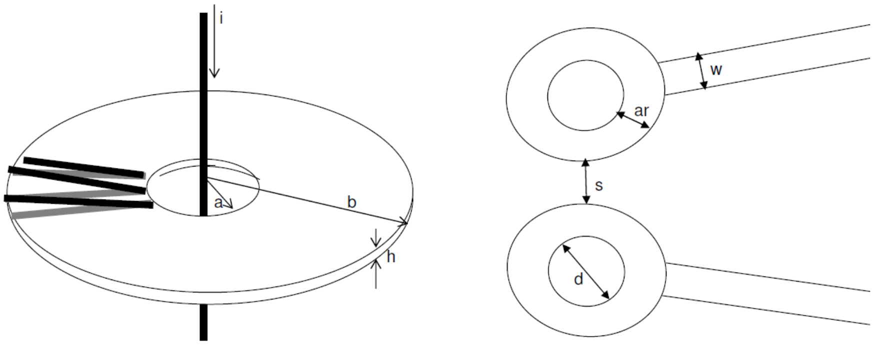

vaccum permability	$\mu 0$	1.25664E-06		
manufacturing specs	mm			cop weight 1 oz
h	0.001575	62 mils		1.4 mils
d	0.000254	10 mils	drill hole	0.03556 mm
w	0.000254	10 mils	track width	
s	0.000152	6 mils	track spacing	
ar	0.000152	6 mils	annular ring	
design parameters				Coil 1 a =
a	0.013970		550 mils	Coil 2 a =
b	0.022225		875 mils	Coil 3 a =
Irms (Nom. Current)	450.00			
ω	376.99 cos(ωt)			

$$\Phi = \frac{\mu_0 I h}{2\pi} \ln\left(\frac{b}{a}\right)$$

$$e = -N \frac{d\Phi}{dt}$$

ϕ	6.5807E-08		
N real	122	N teo	123.4197114
e_{1PCB}	-0.003026654 V	Expected voltage output @ nominal current	
e_{2PCB}	**-0.006053308 V**	**Expected votlage output using 2 pcbs for EMI compensation**	
		Angle	2.950819672
Req level	5 V	Voltage level required. For example, ADE7753 requires 0.3535 volts max	
Gain	825.9946119		
Rg	60.60645643 Ω	For INA128/129	

Figure 2.10 Worksheet showing parameters used for the proposed sensor [19].

Chapter 3: Signal Conditioning

Figure 3.1 illustrates the overall scheme for the signal conditioning system from the RC sensor to the actuator device. The system consists of:

a. The RC sensor device
b. The instrumentation amplifier
c. The active full-wave rectification circuit
d. The zero and span circuit
e. The microcontroller programming device
f. The actuator

The operation of all these devices is explained in the following sections.

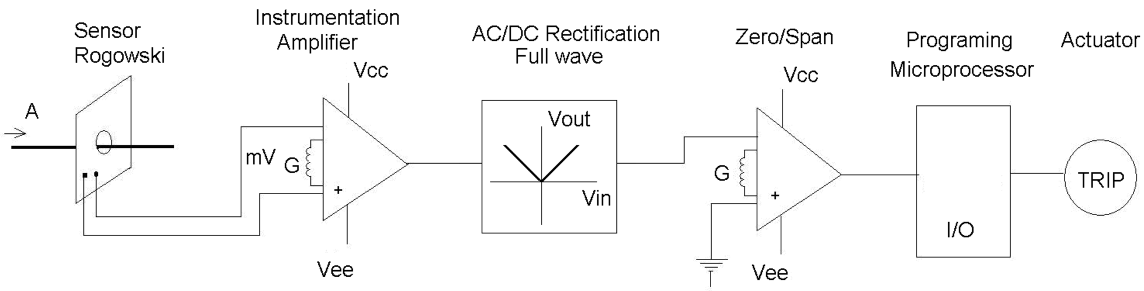

Figure 3.1 Diagram of the overall signal conditioning scheme.

3.1 Operational amplifier operation

The basic function of an operational amplifier is to produce output a signal whose value is directly proportional to the difference between the two input signals. The proportionality factor is known as factor of amplification or gain. The equation that relates the output voltage with the tensions of entry into a circuit with operational amplifier is called the transfer function of the circuit. If the voltage at the entrance with negative sign varies, keeping constant the voltage on the positive input, output voltage will vary with sign opposite to the variation of the negative input; for this reason, the entrance with negative sign called inverting signal. On the contrary, if the voltage on the positive input varies, keeping constant negative input, the output voltage will vary with the same sign that the variation of the positive input, reason why this entry is called non inverting signal. The amplifier only responds to the difference in voltage between the two terminals of input, not to its common potential. With a differential voltage input V_D, the output voltage V_0, will be aV_D, where a is the gain of the amplifier. Both terminals of the amplifier's input are always used regardless of the application. Figure 3.2 shows a simple circuit model of the operational amplifier neglecting high order and frequency limitation effects.

In the ideal case the voltage gain is very large (tends to infinity), the input impedance is also very large (tends to infinite), the bandwidth is very large (tends to infinite), the output impedance is negligible (tends to zero), and the noise is negligible. The output is the difference of the two inputs, multiplied by a gain factor a, as follows:

$$V_0 = aV_D = a(V_P - V_N) \tag{3.1}$$

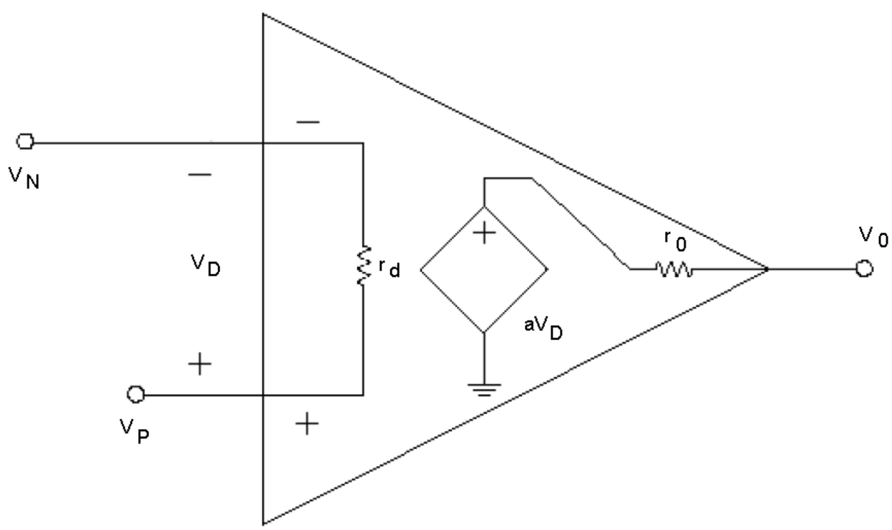

Figure 3.2 Equivalent circuit of an Operational Amplifier [21].

Some negative-feedback configurations used with operational amplifiers are:

1. Non-inverting amplifier.
2. Inverting amplifier.
3. Zero and span circuit.
4. Buffer.
5. Current to voltage converter.
6. Voltage to current converter.
7. Inverter-Adder / non inverter.

An amplification scheme can be used to operate over the non-inverting signal as figure 3.3 shows. A further detailed configuration is given later.

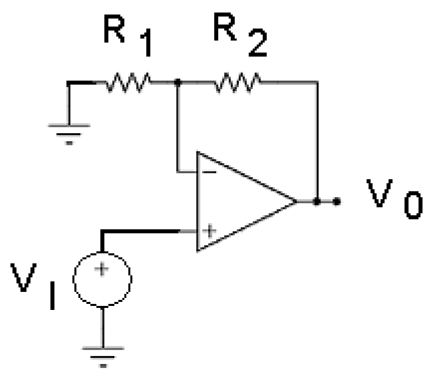

Figure 3.3 Non-inverting amplifier configuration [21].

Some of the op-amp technical characteristics are characterized by: input, output and transfer features. Some common features to consider in the design of a circuit with this type of device are:

a) Input impedance.
b) Maximum differential voltage
c) Input common-mode voltage
d) Compensation of Offset voltage
e) Current compensation
f) Output impedance
g) Slew rate

h) Output current
i) Gain without feedback
j) Common mode rejection factor
k) Bandwidth
l) Response time

3.2 Circuits for signal conditioning

Passing a sinusoidal current for the RC sensor generates a signal (in mV) proportional to this current. Operating range selected for this case was a NEMA starter size 4 with range of full load amperes (FLA) from 45 to 135 A. Within this range, is defined according to the capacity of the motor a current rated FLA. According to the design of the sensor for a value of 45 A, the output sensor in mV is 0.3 mV, and with a input current value of 135 A, the output sensor is 3 mV. This value of voltage in mV will be now passing through the electronic circuit to be able to normalize the signal. Figure 3.4 shows the first part of the conditioning signal including the instrumentation amplifier which has a gain close to 1000. At this time the value of voltage is around 1000 times the output of the sensor and the signal has a sine form amplified according with the gain defined. Figure 3.5 shows the input and output signals form at this stage. Both wave forms are in phase, having different magnitude due gain.

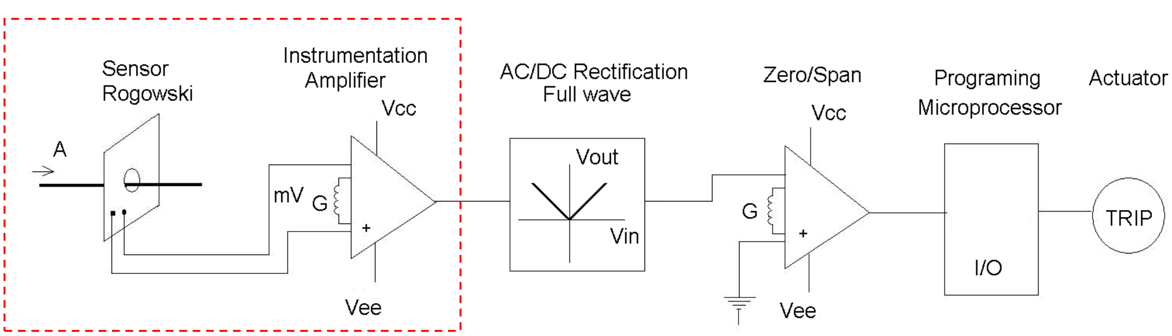

Figure 3.4 First stage of general conditioning system.

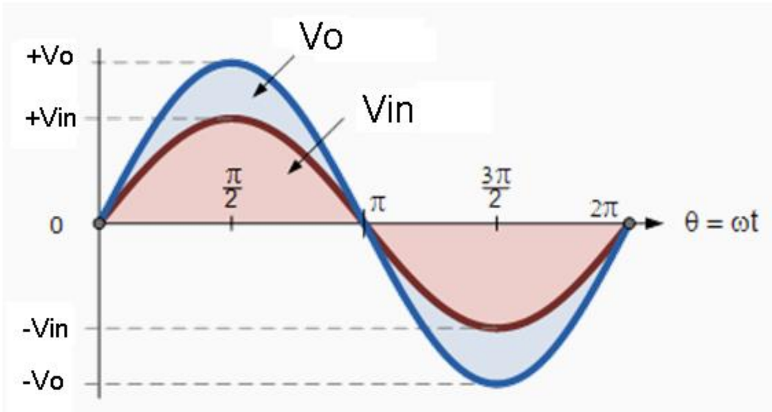

Figure 3.5 Wave form on first stage of conditioning system.

3.2.1 The Instrumentation Amplifier (IA)

The IA is the electronic circuit used in data acquisition applications involving the processing of differential mode voltages. Typical configurations consist of two or three high performance op-amps, resistors, offset calibration networks and protection circuits. The operation performed is the subtraction of the inputs multiplied by a gain factor. The operational amplifier used is the INA129P, which is an integrated circuit device. As shown in figure 3.6, all these devices including the operational amplifiers are included in INA129P. See Appendix I for details on this device.

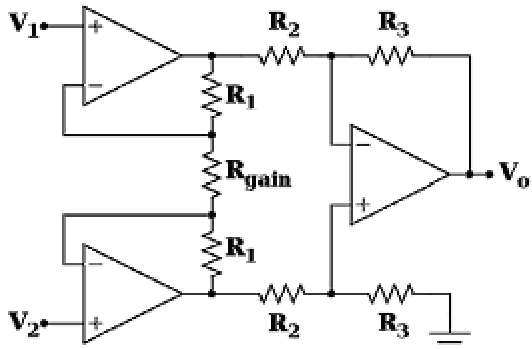

Figure 3.6 Diagram of the proposed IA [21].

The gain of the instrumentation amplifier is:

$$Vo = (V_2 - V_1)\left(1 + \frac{2R_1}{R_g}\right)\frac{R_3}{R_2} \tag{3.2}$$

3.2.2 Full wave active rectifier

The second stage consists of a signal rectifier or an absolute value amplifier circuit. Figure 3.7 shows this stage as a bridge diode rectifier, for this specific purpose a full-wave active rectifier with a filter is used for removing the ripple coming from the RC coil. This stage was developed using an operational amplifier type LM324N. See Appendix for technical details of this device. The output signal of this stage is shown in figure 3.9.

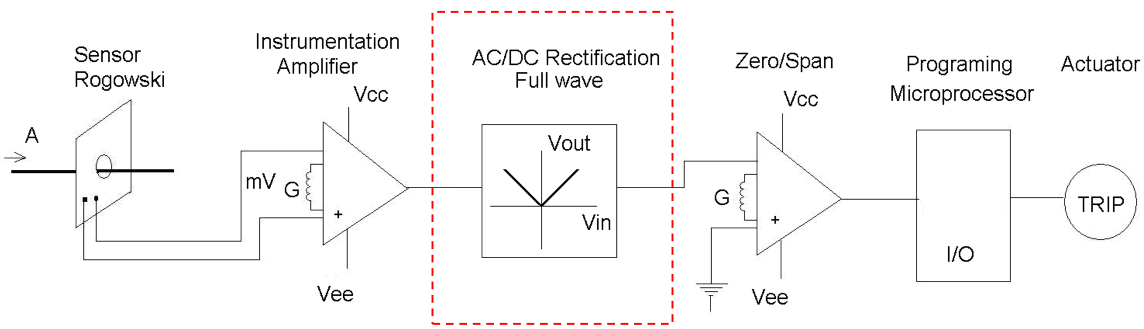

Figure 3.7 Second stage of general conditioning system.

A full wave active rectifier produces a complete positive output which is the absolute value of the input sine signal wave form V_{in}. There are two half wave rectifiers. The upper part operates with the positive portion of the input; only the positive input sine signal is inverted and forms the negative part V_1. The below part operates with the negative portion of the input, only the negative input sine signal is inverted and forms the positive part V_2. The output is summed with proper polarities to get the rectified signal V_o as figure

3.8 shows. The output signal is not uniform due specific features of the op amp device. As final part of the rectifier circuit there is a C element connected in parallel with the output signal to get eliminated the ripple effect as figure 3.9 shows.

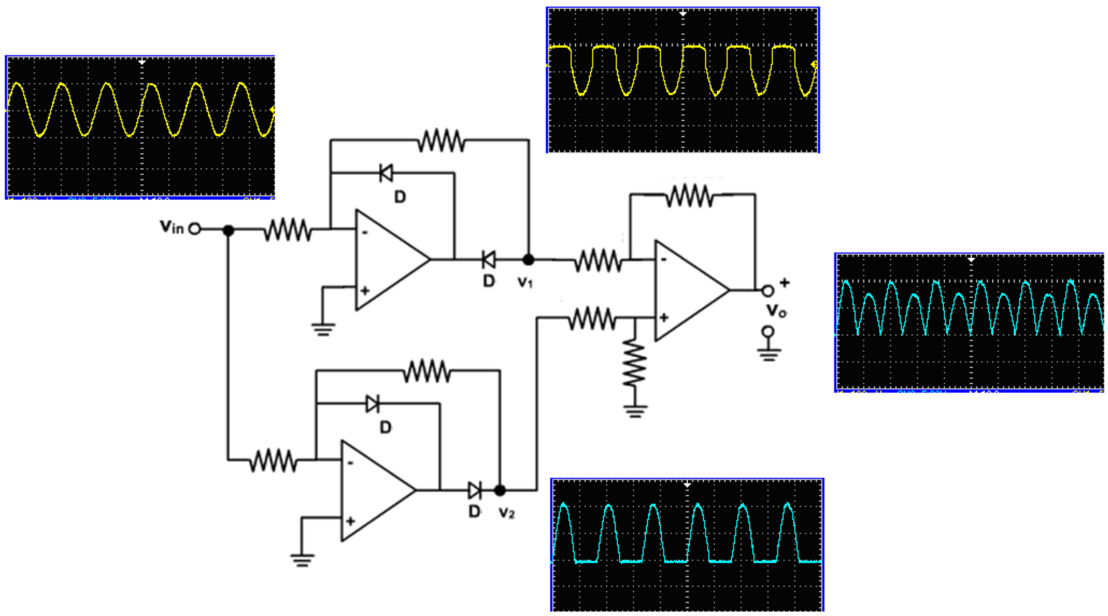

Figure 3.8 Active rectifier diagram.

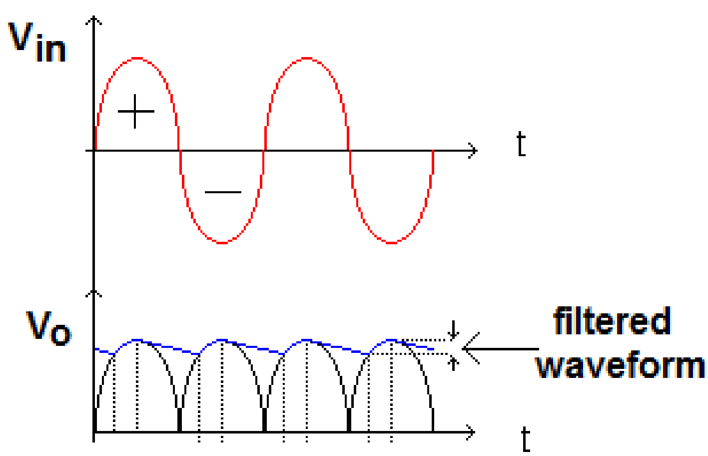

Figure 3.9 Wave forms for the active rectifier amplifier.

3.2.3 Zero and Span Circuit

The third stage is the zero and span adjustments to secure the offset with the gain required to have the range of analog signal from 0 to 5 V DC. The span setting is used to change the slope or gain of the curve between the input and output signals. The zero setting is used to produce a parallel change between input and output signal without changing the slope. Figure 3.10 shows the zero adjustment to get the offset desired, and shows the span adjustment to get the gain desired.

The calibration of an analog signal coming from a sensor or a transducer involves the adjustment of the span (gain) and zero (offset) using a voltage amplifier. The adjustment is reached using variable resistors devices, when zero and span are adjusted using the same variable resistor there is an effect on the other, the gain changes alter the zero point. Separate variable resistors are needed, the setting of one of them is not enough only to have the correct value; a linear function is used to express these values. Figure 3.11 shows the third stage of conditioning signal.

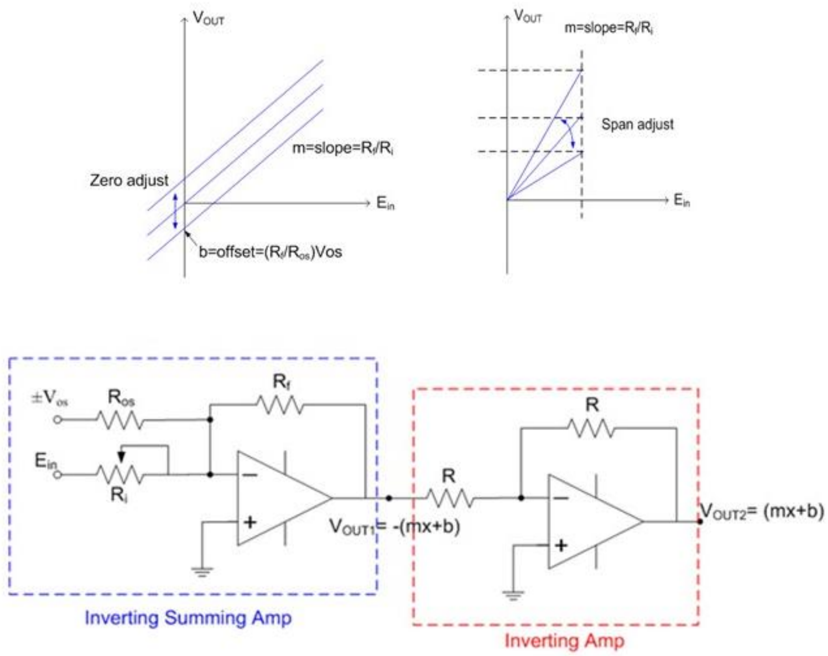

Figure 3.10 Typical zero span adjustment circuit [20].

When the input current in the sensor is 0 Amp, the value expected in this stage should be 0 VDC. For this project it was taken as a nominal current value of 45 Amp. The expected signal with this nominal current of 45 Amp is 0.50 VDC according range of 0-5 VDC calculated using equation 3.4. Figure 3.12 shows an I-V conversion line with these values.

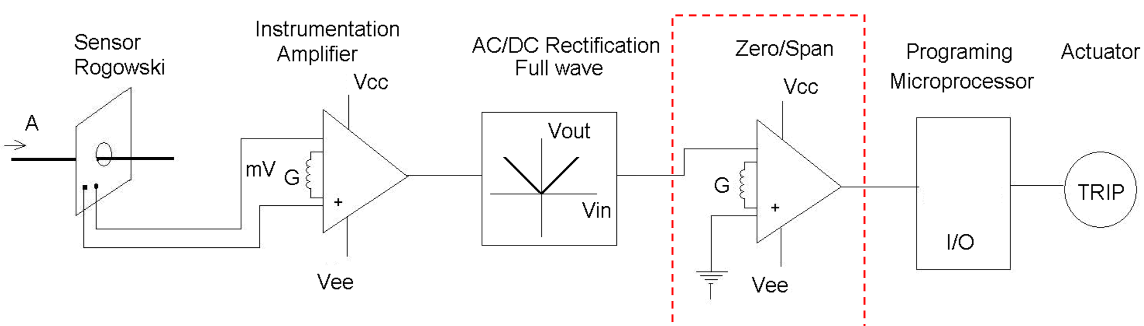

Figure 3.11 Third stage of general conditioning system.

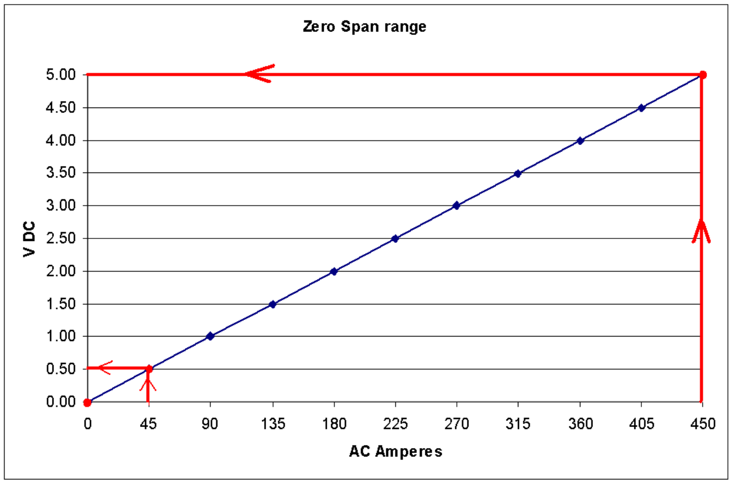

Figure 3.12 Proposed Zero span range conversion from I to V.

Table 3.1 shows the zero span range provided by the circuit from figure 3.10. The maximum 5.00 VDC corresponds to a value of 450 A in the sensor, and the nominal current of 45 corresponds to a value of 0.50 VDC. The curve has a slope m value which is defined by equation 3.3; Figure 3.12 shows the zero span linear curve.

Table 3.1 Ideal value of zero and span range from I to V.

IDEAL VALUE ZERO SPAN	
Amp	V DC
0	0.00
45	0.50
90	1.00
135	1.50
180	2.00
225	2.50
270	3.00
315	3.50
360	4.00
405	4.50
450	5.00

Having 2 points of curve (0, 5) and (450, 0), it can be defined m as follows:

$$m = \frac{y2 - y1}{x2 - x1} = \frac{5 - 0}{450 - 0} = 0.0111 \quad \frac{V_{DC}}{A_{AC}} \tag{3.3}$$

Using general curve of 2 points $y = mx + b$, and having defined m value, equation of zero span curve is defined as follows:

$$y = 0.0111x + b \qquad V_{DC} \tag{3.4}$$

y = vertical position in curve expressed in V_{DC}

x = horizontal position in curve expressed in A_{AC}

m = slope or span expressed in $\frac{V_{DC}}{A_{AC}}$

b = point of intersection, or zero, between the curve and the axis 'y',

where b is 0, expressed in V_{DC}

For signal conditioning system, this stage was developed using an operational amplifier type LM324N. See Appendix for technical reference.

3.2.4 Microcontroller functions

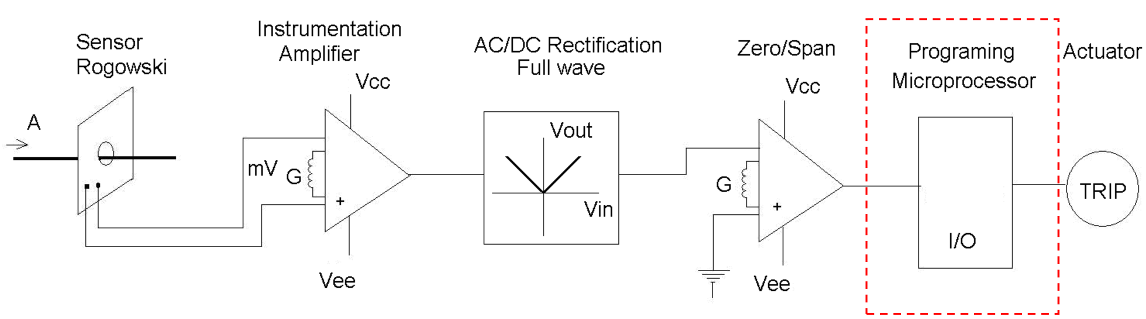

Figure 3.13 Fourth stage, the microcontroller device.

Figure 3.13 shows the fourth stage which is related to the microcontroller functions. The output from 0 to 5 V DC is the analog signal coming from the zero and span circuit and it will be converted in digital signal into the microprocessor, this signal will be scheduled according to the logic for the conditions of overload, unbalance and loss of phase. The nominal current value will be the basis for the calculation of overload, unbalance and loss of phase to be able to have the trigger to the actuator signal. The behavior of the relay based on the current against response time will be based on class 20 curve trip, it is expected that in 20 seconds or less to a value of 6 times the nominal current value operates the overload relay.

For programming purposes, the logic conditions are described below and the C language programming code is included in Appendix section. Figure 3.14 shows a flow diagram for all trip conditions; over current, unbalance and phase loss. The trip signal can be reached for each of these trip conditions. An ATMEGA168 controller was used to get these conditions programmed.

3.2.4.1 Over-current trip condition.

The current range for the sensor was defined from 0 to 450 A. With this current the output voltage signal from the sensor was conditioned to get in zero span stage the 0 to 5 VDC output signal which is the input to the microcontroller device. The range takes the 0 value to get input signal for phase loss trip condition. Full load amperes (FLA) for this sensor was defined as 45 A, with the maximum value of 10*FLA, 450 A. According zero span stage, the output signal is adjusted as Table 3.2 shows:

Table 3.2 Signal conditioning for Input RC signals.

Input current to RC sensor (Amps, rms)	Output of the zero and span circuit (Vdc)
0	0
450	5

The FLA in sensor is defined as 45 Amp. The zero span value expected for 45 A. is 0.5 VDC. These are the current and zero span nominal values of the sensor. The overload protection is based on a three phase system. There is a sensor per phase A, B and C. Each sensor has their independent conditioning signal since instrumentation amplifier to zero span stage. Every sensor A, B and C has their input current and their output voltage signal connected to each A, B and C conditioning stage. The three phase output zero span signals which have values from 0 to 5 VDC are connected to the microcontroller device in order to get the trip signal with the actuator unit. The microcontroller device was programmed based on the described trip conditions and following the flow diagram shown in figure 3.14.

There is an output voltage value with a magnitude between 0 to 5 VDC per phase which are named for programming purposes as A, B and C. There is an internal process in the microcontroller to define what phase A, B or C has the maximum value as Table 3.3 shows. The maximum value is named as H. Comparison process and H value are defined as follows:

Table 3.3 Conditional table for high current trip.

Main condition	Primary results (then)	Secondary condition (else)	Secondary result (then)	Tertiary result (else
If A>B and A>C	Then H=A			
		Else If B>C and B>A	Then H=B	
				Else H=C

The overload protection system based on curve class 20 starts working at 1.25*FLA, above or equal of this value there is a specific time to get a trip signal due over current condition. Taking as nominal current of 45 A, the overload protection starts at 1.25*FLA, which is 56.25 A, and the zero span output value expected is 0.63 VDC. The required equations to establish those conditions are:

$$\text{FACTOR}= (H/0.0111)/45 \tag{3.5}$$

$$\text{TIME}= 1680*\text{FACTOR}^{(-2.7)} +6 \tag{3.6}$$

Where TIME is in seconds. Table 3.4 shows these conditions to start overload protection due high current condition. FACTOR is evaluated using equation 3.6 to get TIME (which is the time to get a trip signal), in this case over current. If trip time is not completed, there is a reset in TIME.

Table 3.4 Condition to high current process class 20

Main condition	Primary results (then)	Secondary results (then)
IF H>1.25FLA (56.25 amp, 0.63 VDC)	FACTOR= (H/0.0111)/45 Equation 3.5	TIME= 1680*FACTOR^ (-2.7) +6 Equation 3.6
	FACTOR is the multiples of FLA.	TIME in seconds.

3.2.4.2 Unbalance trip

As mentioned in over current condition, A, B and C were defined based on the output voltage values with a magnitude between 0 and 5 VDC per phase. There is an internal process to define the average between A, B and C named as AV. Then a deviation process was developed for each phase named as DEVA, DEVB and DEVC to define the maximum deviation between each phase and average value. This deviation will determine the unbalance percent as UNB. An unbalance trip signal exists when UNB is grater or equal to 25 % during 3 seconds. The following procedure is defined to get unbalance trip signal:

$$AV= (A+B+C)/3 \tag{3.7}$$

$$DEVA=ABS\ (A-AV) \tag{3.8}$$

$$DEVB=ABS\ (B-AV) \tag{3.9}$$

$$DEVC=ABS\ (C-AV) \tag{3.10}$$

$$DEVMAX=MAX\ (DEVA, DEVB, DEVC) \tag{3.11}$$

$$UNB=100(DEVMAX/AV) \tag{3.12}$$

IF UNB >= 25 %, on 3 seconds

3.2.4.3 Phase loss

As mentioned in over current condition, A, B and C were defined based on the output voltage values with a magnitude between 0 and 5 VDC per phase. There is an internal procedure to define if one of these values A, B or C is equal to 0. When this condition exists during 3 seconds there is a phase loss trip signal. Or if the average value named as AV is equal or less than 25 % of FLA during 3 seconds a phase loss trip signal is present. The FLA is defined as 45 A. with a zero span value of 0.5 VDC. The following procedure gets the unbalance trip signal:

If (A, B, or C =0) during 3 seconds

or

If AV =< 25 % of FLA (45 amps= 0.5 VDC) during 3 seconds

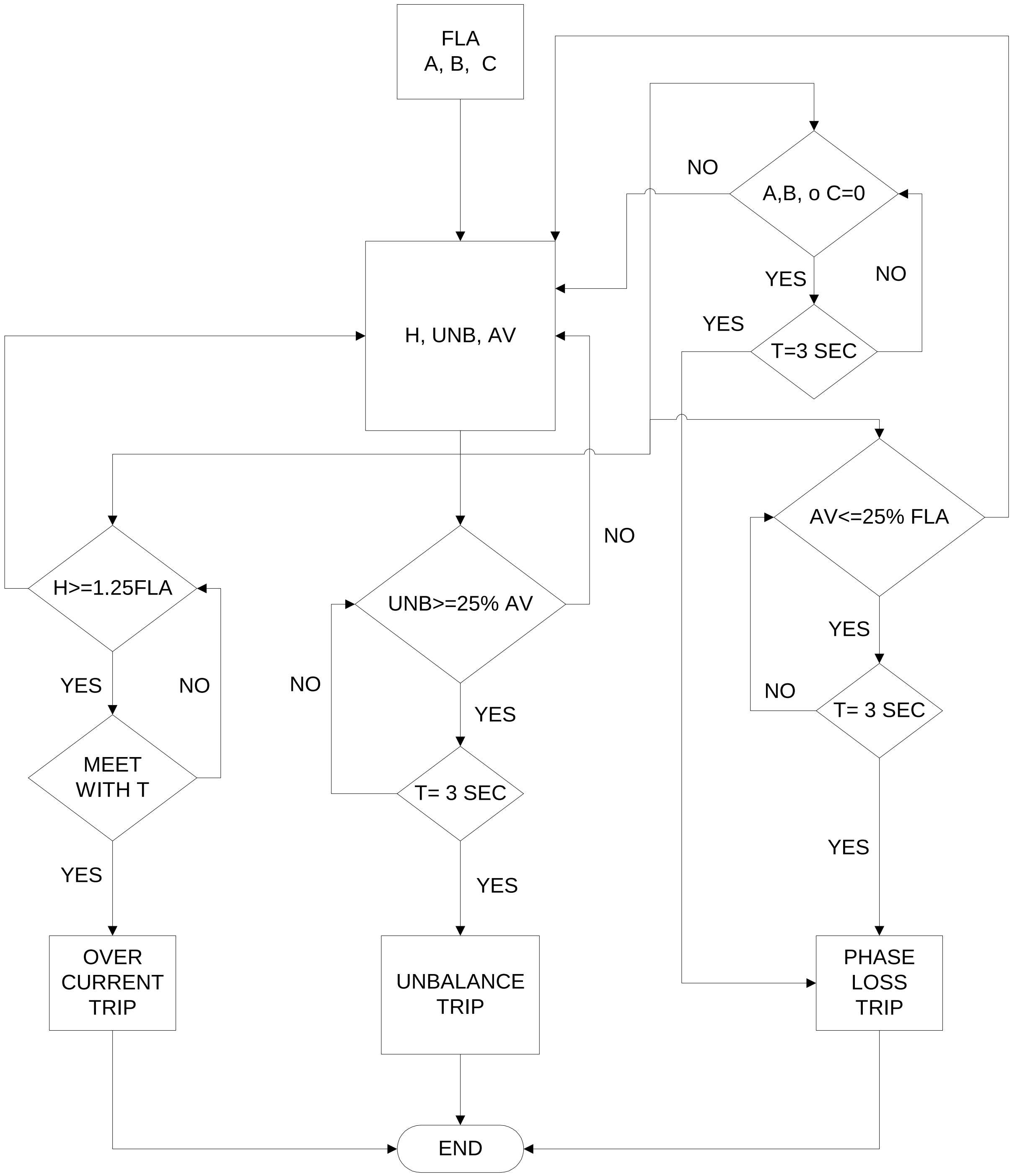

Figure 3.14 Flow diagram for trip conditions.

3.2.5 Actuator

Figure 3.15 shows the last stage of action circuit which consists in sending the signal from microprocessor to the actuator when a trip signal occurs as an over current, unbalance or phase loss based on the logical conditions. There is an output voltage (5.00 VDC) signal coming from the microprocessor when a trip signal is present. An optocoupler device as figure 3.16 shows is used to transfer this signal between microprocessor and actuator isolated circuit. The signal coming from the microprocessor energizes the led circuit into the optocoupler device. See figure 3.17 shows an optocoupler diagram. As part of the actuator circuit, there is a TIP device (power transistor NPN type which usually uses a Darlington´s type configuration) connected after phototransistor, when a trip signal is present the actuator control circuit is energized throw the TIP device, thus the normal closed contact (95-96) on overload relay unit changes to open position, and then the power circuit is de energized having the power off in the motor and it is protected for any of the three conditions possible. Figure 3.18 shows the complete diagram including optocoupler with TIP device wired to actuator.

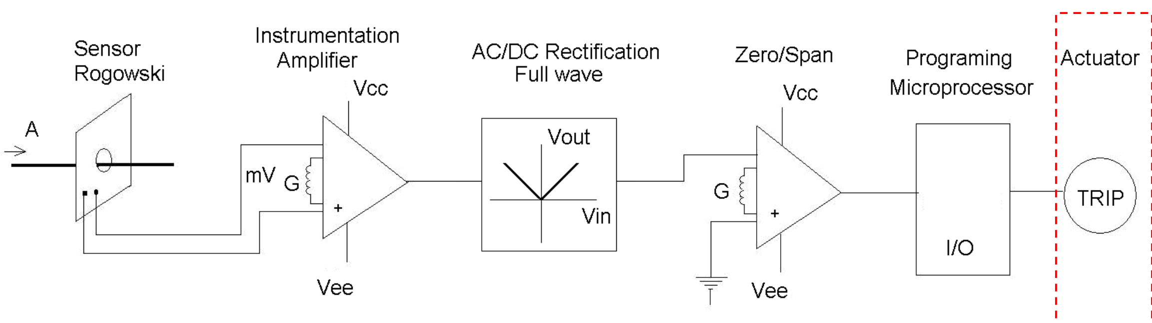

Figure 3.15 Actuator stage.

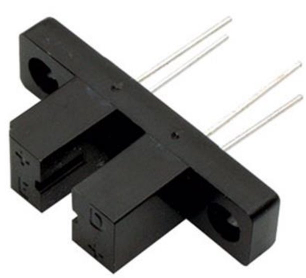

Figure 3.16 Optocoupler device.

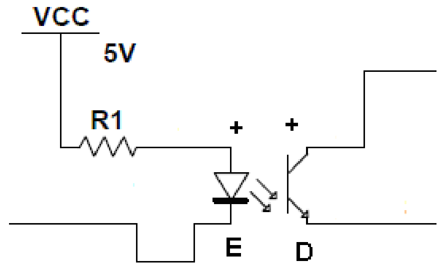

Figure 3.17 Optocoupler diagram.

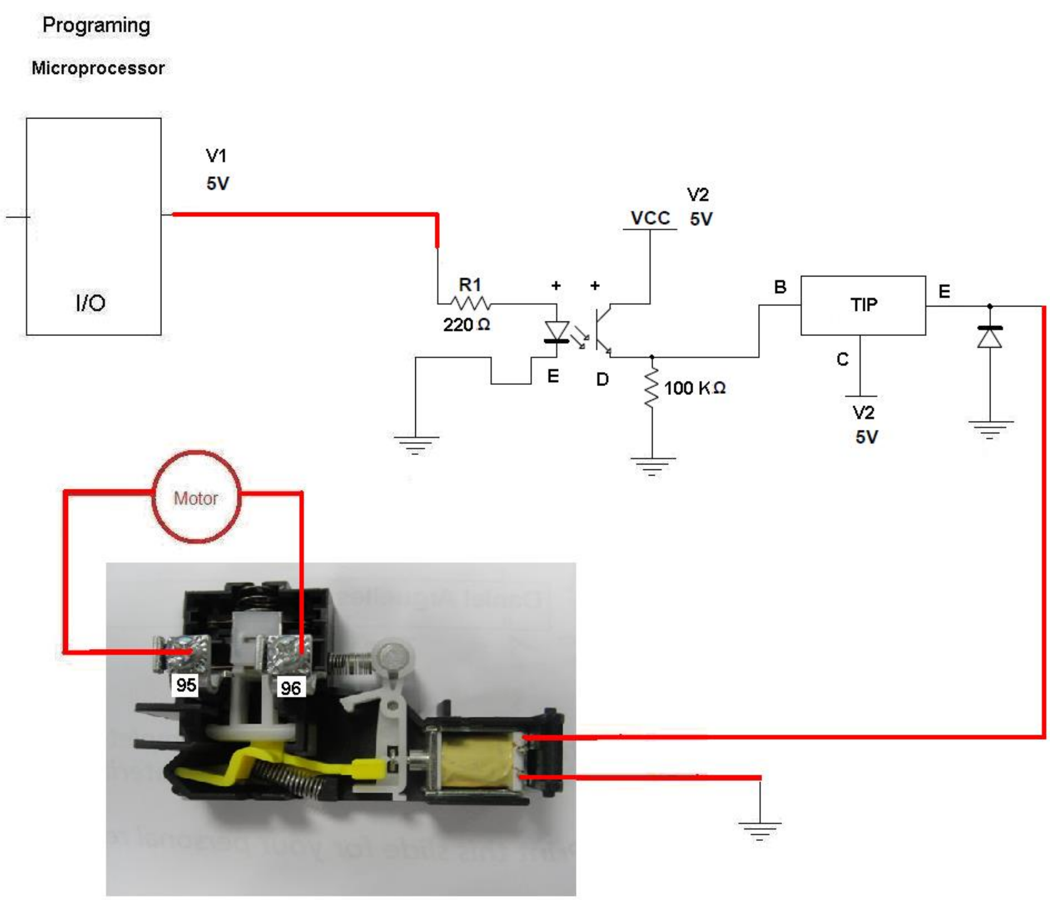

Figure 3.18 Actuator with optocoupler diagram.

In this prototype we used the actuator device shown in Figure 3.19 which is part of the actual solid state overload relay shown in Figure 3.20. When the actuator is energized, it releases a mechanism to change contacts position from close to open. These terminal contacts are identified as 95-96 for reference purposes.

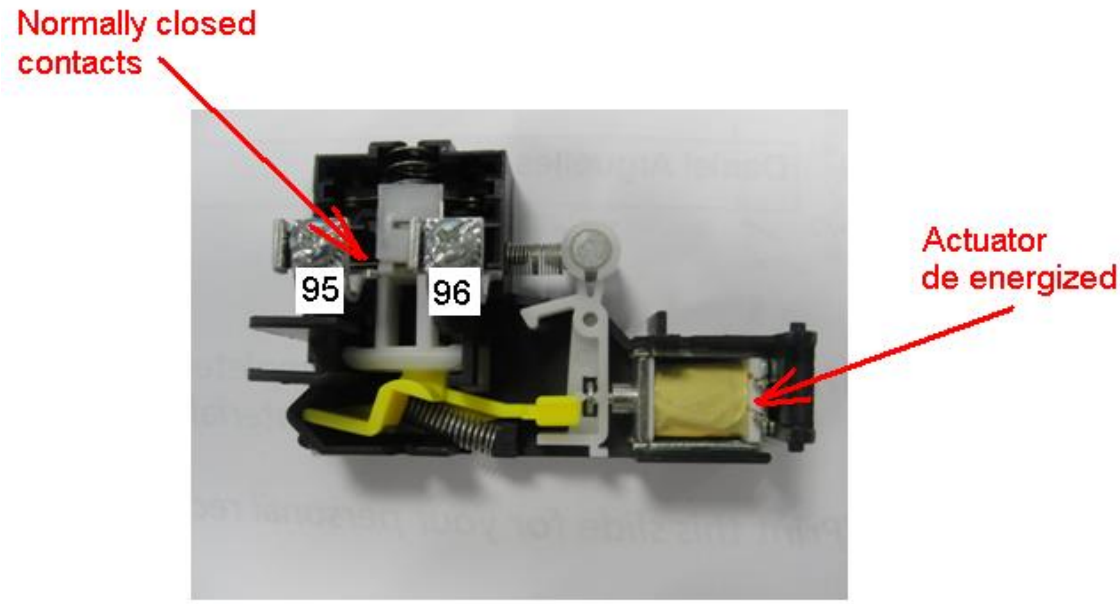

Figure 3.19 Actuator used in solid state over load relay.

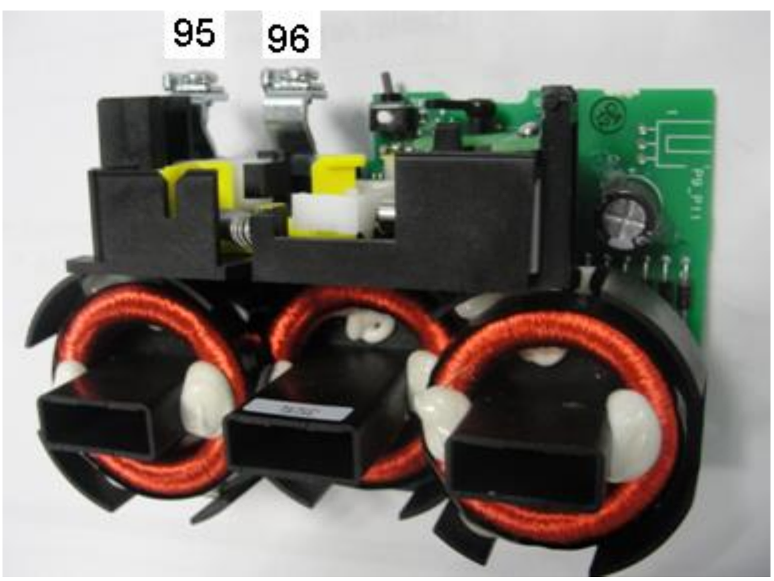

Figure 3.20 Actuator mounted over CT carrier.

Chapter 4: Prototype of Overload Relay using the RC System.

4.1 Prototype description

Based on the solid state overload relay shown in Figure 4.1, the proposed RC sensor was developed. From the typical overload relay system, CTs, the electronic PCB unit and the actuator relay were disassembled, leaving only the CT carrier as shown in both, Figures 4.1 and 4.2. According to parameters defined in Chapter 2 the new PCB sensor was designed which now includes the RC system.

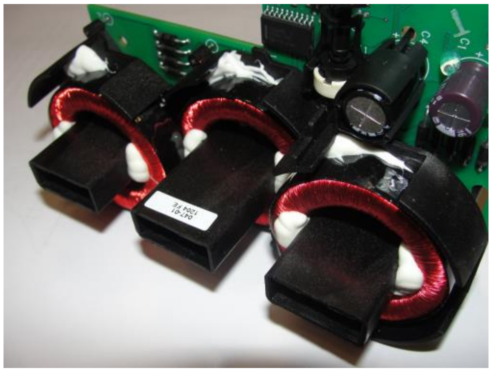

Figure 4.1 Solid state overload relay.

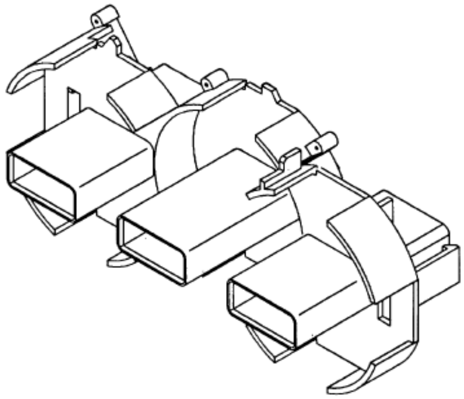

Figure 4.2 Solid State over load relay CT carrier.

As part of the design process, the PCB unit was developed using Altium software [29]. The Figure 4.3 shows the PCB detail of the RC sensor system. The design illustrates symmetrical concentric traces which initiates at one side (blue traces) and finalizes at the other side (red traces). The small concentric traces are connected side by side through vias which penetrates the PCB structure.

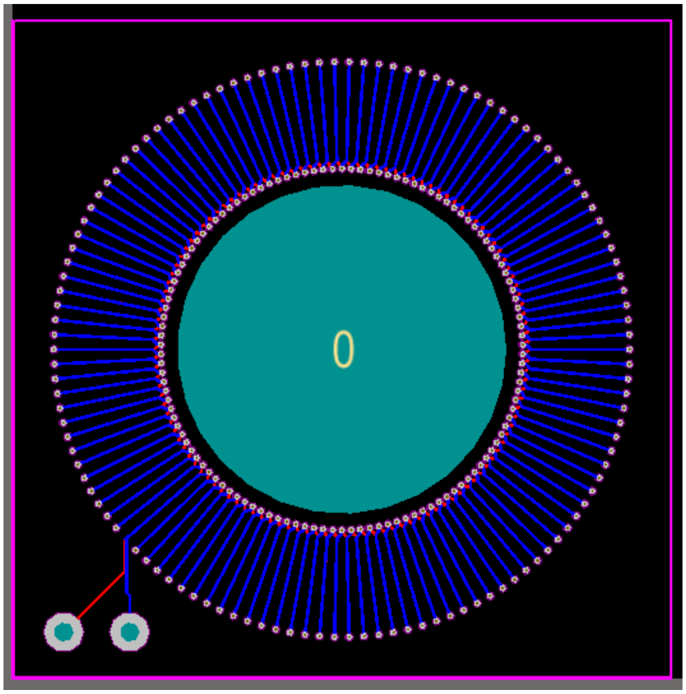

Figure 4.3 PCB sensor design on Altium software.

Figure 4.4 shows how RC-PCB sensors were manufactured and installed in the CT carrier taken from the solid state overload relay. This assembly was only to verify if the proposed sensor fitted in the CT carrier. One PCB was installed on carrier to develop linearity, gain and rectifier isolated tests (only one sensor with their electronic conditioning signal according stage). These tests were developed to ensure sensor was manufactured according design requirements, and verify the electronic conditioning signal circuit works correctly.

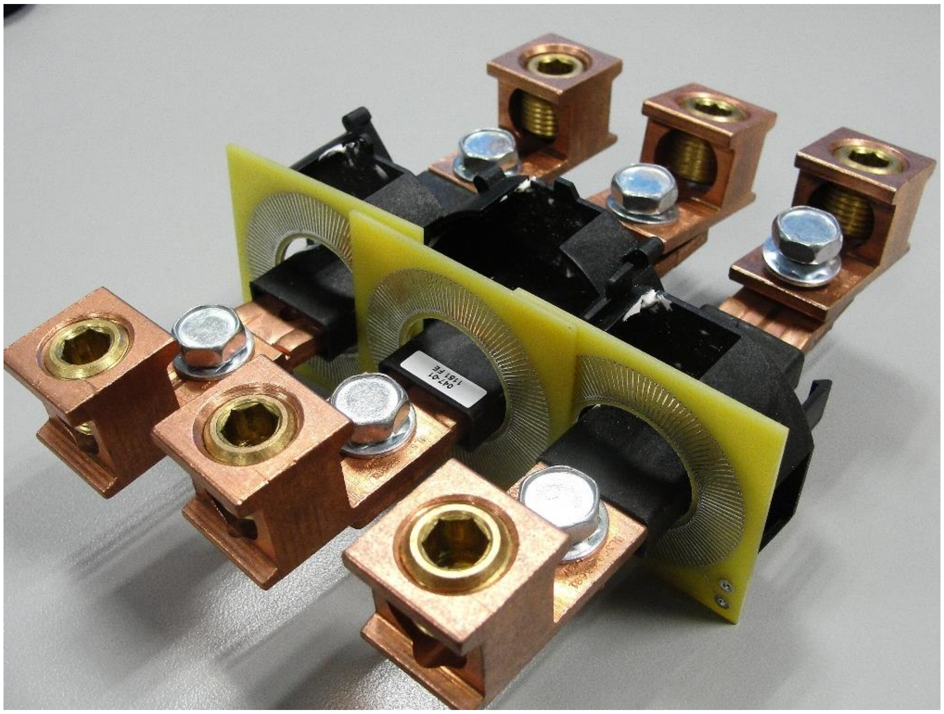

Figure 4.4 CT carrier with RC-PCB sensors installed.

4.2 Simulations

The Electronic circuits for conditioning signal were simulated and validated using Multisim software [30]. Figure 4.5 shows the instrumentation amplifier diagram.

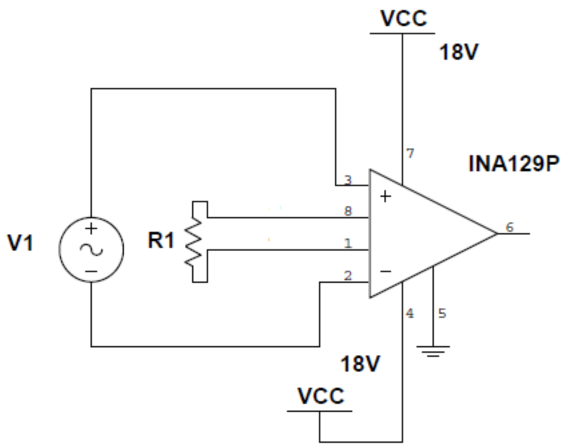

Figure 4.5 Instrumentation amplifier circuit diagram.

Figure 4.6 shows the rectifier circuit diagram that consists of two active rectifiers (positive and negative) and a differential amplifier which receives their outputs to generate an absolute value operation over the input signal.

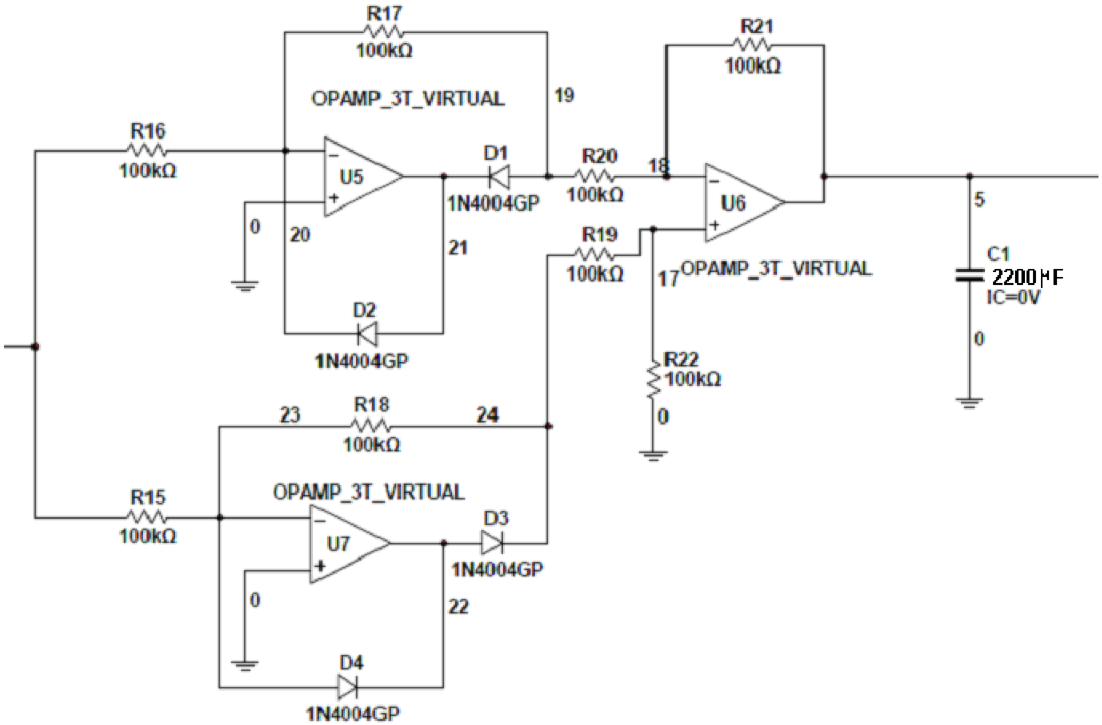

Figure 4.6 Active rectifier circuit diagram.

Figure 4.7 shows the zero span circuit that consists of a non-inverting amplifier and a set of three inverting amplifiers. The resulting voltage transfer curve (VTC), similar to the one shown in figure 3.10, is obtained by calibrating the feedback potentiometer for the middle inverting amplifier (sets the gain) and the input potentiometer (sets the offset) of the input inverting amplifier. Results of tests performed on the signal conditioning circuits are described in the following sections.

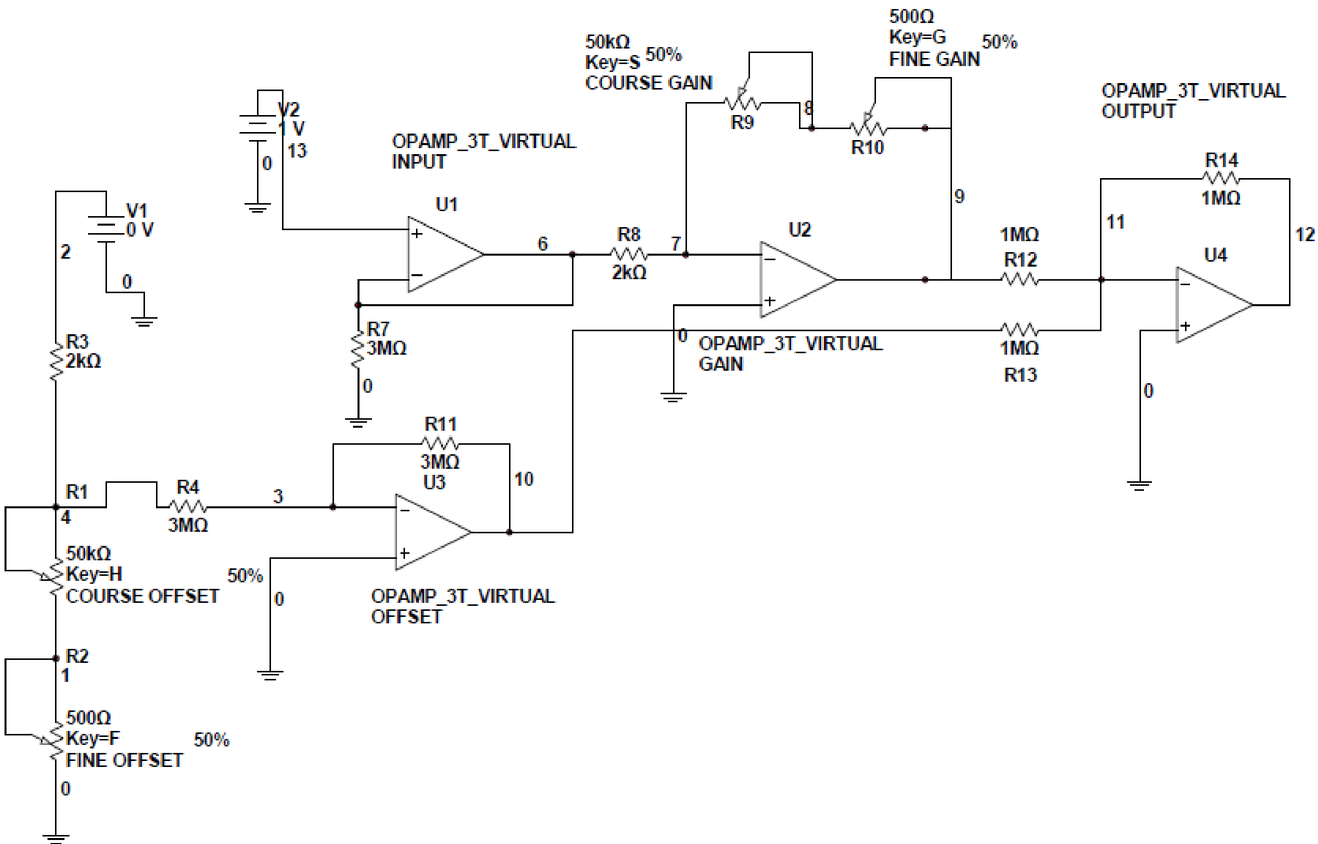

Figure 4.7 Zero span circuit diagram.

Figure 4.8 shows the optocoupler and the actuator circuits diagram. Again the testing from isolated and integrated tests for this part of the circuit is presented in the following sections.

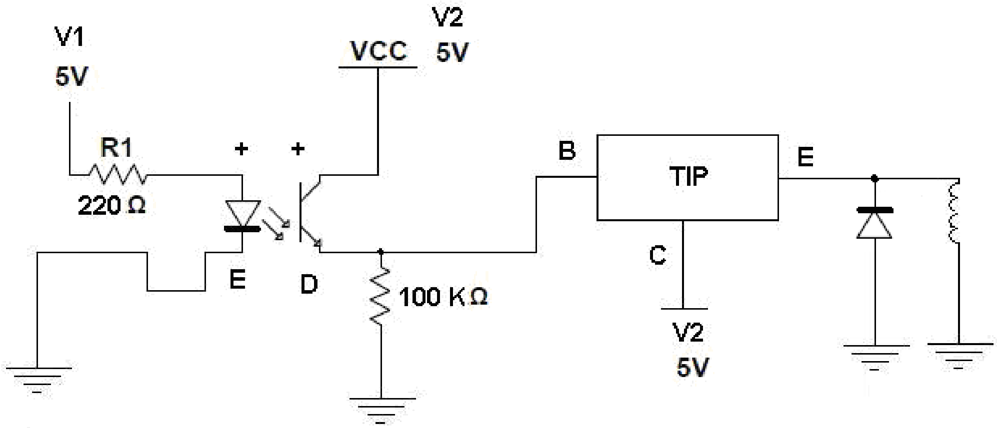

Figure 4.8 Optocoupler and actuator circuits diagram.

4.3 Isolated tests

Individual device components were tested to ensure the robustness of the electronic hardware associated to the RC sensor device. Isolated tests on the following electronic circuits were performed: instrumentation amplifier, active rectifier, and zero and span amplifier.

4.3.1 Calculated Gain

Gain was defined based on a precision, low power instrumentation amplifier device INA 129 which has a symmetrical array of three op-amp design. See Appendix I for further technical details. To setting the gain a variable resistor R_G was connected on terminals 1 and 8 as is shown in figure 4.9.

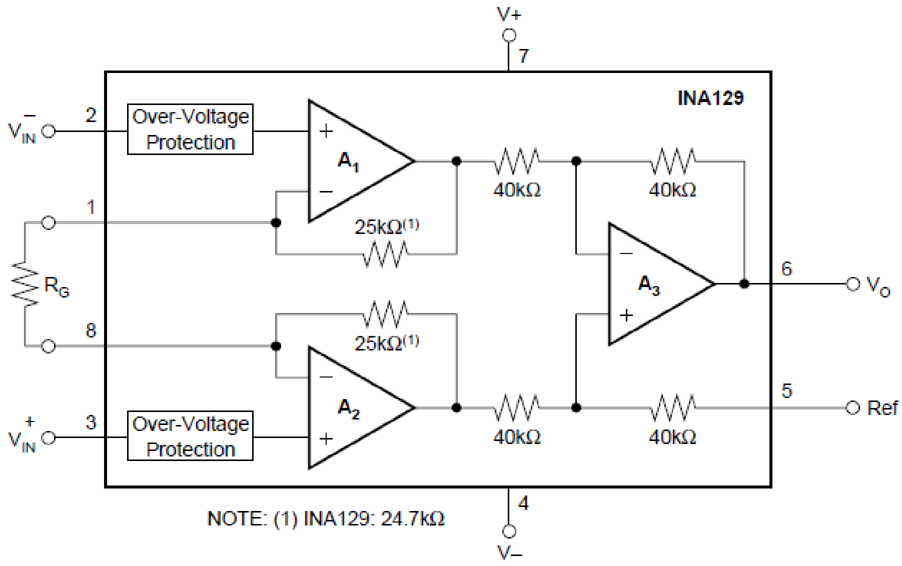

Figure 4.9 INA129P Instrumentation Amplifier connection diagram.

The amplifier gain G is given by:

$$G = 1 + \frac{49.4K\Omega}{R_G} \tag{4.1}$$

Output voltage from sensor was connected to terminals 2 and 3 in instrumentation amplifier to get V_{IN} signal according Figure 4.9. R_G was adjusted to get a gain value as table 4.1 shows, thus having an output voltage V_0 amplified for the next stage.

Table 4.1 Instrumentation amplifier output.

Input Current sensor	Output voltage sensor (mV)	Instrumentation amplifier output (mV)	Gain
45	0.4	190	475
90	0.7	335	479
135	1	500	500
180	1.3	670	515
225	1.6	845	528
270	1.9	1020	537
315	2.2	1200	545
360	2.5	1350	540
405	2.8	1520	543

450	3.1	1710	552

4.3.2 Linearity Test

Linearity test was developed using a single sensor passing a power cable throw the sensor and the cable connected to the current source as figure 4.10 shows. An AC current range from 45 to 450 A. was injected to the circuit; the output voltage from the sensor was measured using an AC voltmeter. Table 4.2 shows the output voltage measured and their comparison with theoretical value obtained from design. Values of mV range were obtained, as expected. A difference between real and theoretical values was found, this error was about 10% in most of the current measurements. Significant error differences are expected to be improved during zero and span stage. Figure 4.11 shows the current to voltage transfer test (I-V) to verify the linear behavior of the sensor.

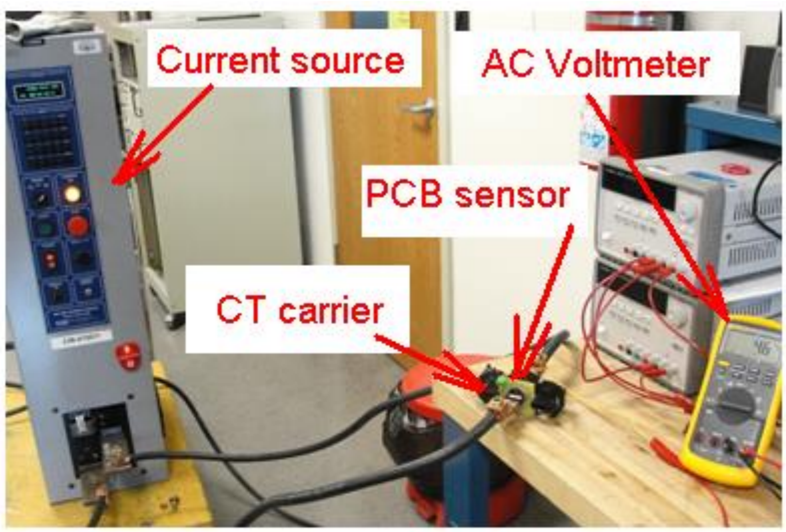

Figure 4.10 Single phase sensor test developed.

Table 4.2 Linear response I-V conversion results compared with design of RC-PCB sensor.

Input current Amp	Output voltage designed mV	Output voltage measured mV	Error %
45	0.3	0.4	25.0
90	0.6	0.7	14.3
135	0.9	1	10.0
180	1.2	1.3	7.7
225	1.5	1.6	6.3
270	1.8	1.9	5.3
315	2.1	2.2	4.5
360	2.4	2.5	4.0
405	2.7	2.8	3.6
450	3.0	3.1	3.2

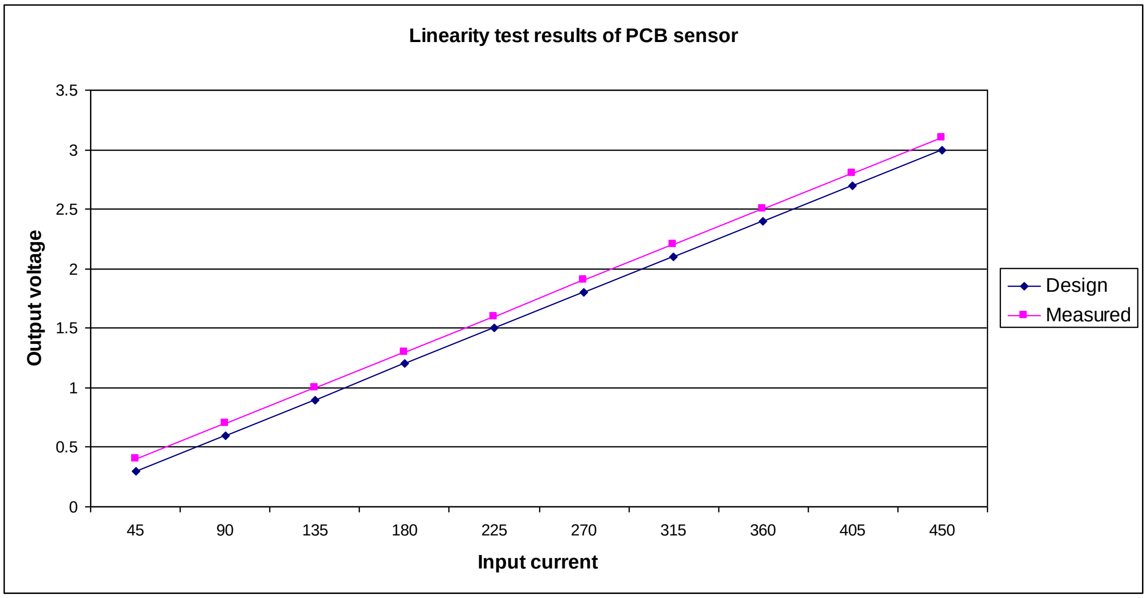

Figure 4.11 I-V (zero and span) transfer test resulting graph.

4.3.3 Rectified signal test

Test was developed using a single sensor, the current source, instrumentation amplifier stage, and the rectified conditioning stage connected to the sensor. Table 4.3

shows the results of this rectified signal stage. A capacitor device was used to get eliminated the ripple effect on the output signal and gives a nearly constant DC signal. Figure 4.12 and 4.13 show the output signal with and without the capacitor. There is about less than 6 % between the output voltage coming from the sensor and the rectified output signal. This difference is due the filter and the capacitor charge process, these losses are expected to be improved during zero and span stage. A capacitor element was connected in parallel with the output signal coming from the rectifier circuit in order to perform a filtering function. The value of C element was defined with the results of some tests according output signal behavior shown in oscilloscope monitor. The capacitor element was defined as 2200 µf.

Table 4.3 Rectified signal mV DC.

Input Current sensor	Output voltage sensor (mV)	Instrumentation amplifier output (mV , AC)	Gain	Rectified signal (mV, DC)
45	0.4	190	475	188
90	0.7	335	479	328
135	1	500	500	490
180	1.3	670	515	660
225	1.6	845	528	820
270	1.9	1020	537	990
315	2.2	1200	545	1150
360	2.5	1350	540	1280
405	2.8	1520	543	1460
450	3.1	1710	552	1650

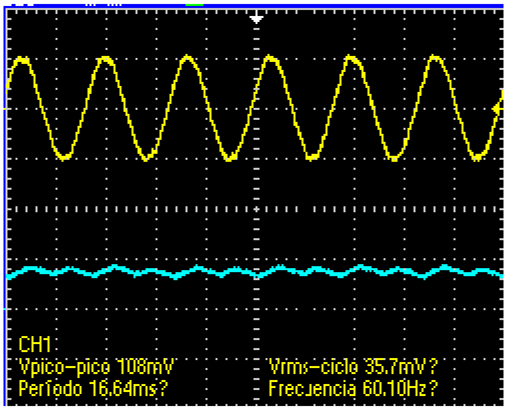

Figure 4.12 Output signal rectified with capacitor element.

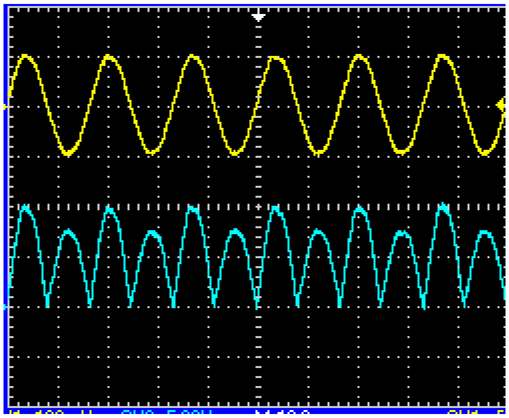

Figure 4.13 Output signal rectified full wave without capacitor element.

Figures 4.14 show detail of the full wave active rectifier process. As was described in section 3.2.2, the circuit was developed using 3 op amps devices, there are two of them which are connected to the input voltage signal, one of these works only with the positive sine signal, the other works only with the negative sine signal and the last op amp take these two signals and develop the adding process. Figure 4.15 shows a manual adjustment on the screen to get both signals together before the adding process. The adding process was shown in Figure 4.13.

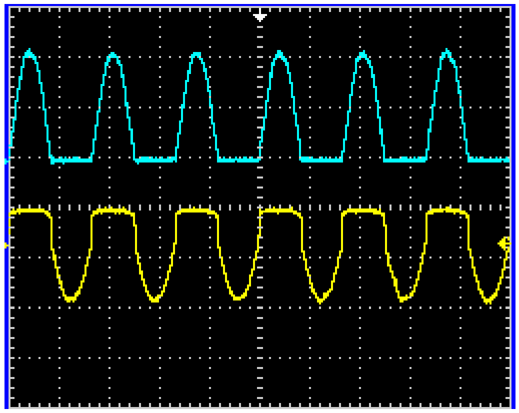

Figure 4.14 Signal rectified half wave 1-2 with out capacitor element.

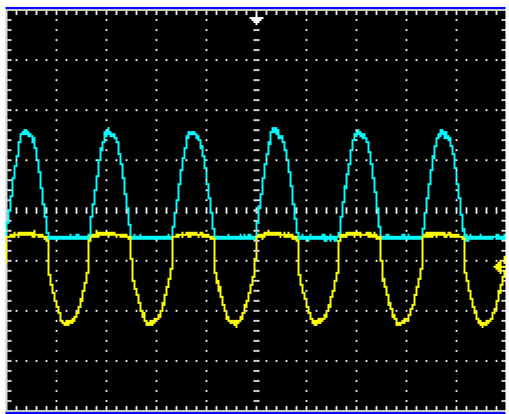

Figure 4.15 Signal rectified half wave 2-2 with out capacitor element.

4.3.4 Zero span adjustment and results

These values were taken from a single phase sensor device connected throw a current source. All electronic stages were connected in order to get the complete conditioning signal, and for this case review the zero span stage. At 0 A. the output DC voltage required should be 0 VDC, and for 450 A. the value expected should be 5 VDC in order to get the 0-5 VDC range required for the microprocessor unit. Table 4.4 and figure

4.16 show the ideal and practical results using an I-V transfer curve. The curve shows a slight hysteresis effect from 90 to 135 A and from 360 to 405 A.

Table 4.4 Real values of the I-V conversion.

I-V conversion test	
Amp	**V DC**
0	0.00
45	0.40
90	0.86
135	1.38
180	1.92
225	2.45
270	2.96
315	3.47
360	3.90
405	4.41
450	5.00

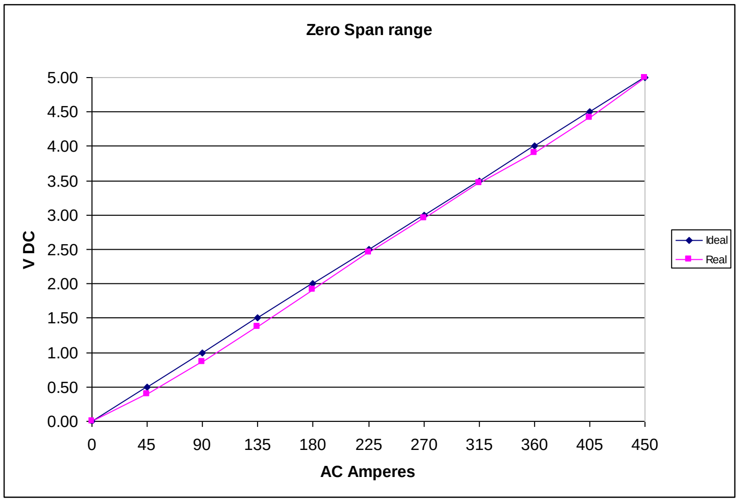

Figure 4.16 Ideal and real I-V (zero and span) behavior of the working prototype.

Figure 4.17 shows the instrumentation amplifier signal in color blue, rectified signal in yellow and zero span output in color magenta.

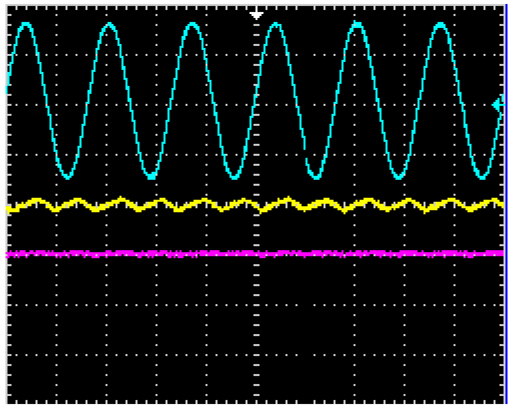

Figure 4.17 Output of instrumentation amplifier, rectifier and zero span signals.

Initially an external source was used to simulate the output voltage of the sensor. This supply was limited by lower limit of 10 mV. The output voltage required by design was 0.3 to 3 mV. A voltage divider was developed in order to have this voltage range. This voltage divider was removed sensor was tested with the full circuit.

Part of the isolated tests started without the sensor, and using amplifier instrumentation was built with resistors and some op-amps. Several issues were presented as not enough gain, and resistors do not have the same values (tolerances), this cause noise and not stable signal.

As was mentioned before, the adjustment of zero and span are reached using variable resistors devices, when zero and span are adjusted using the same variable resistor there is an effect on the other, the gain changes alter the zero point. Separate variable resistors are needed, the setting of one of them is not enough only to have the correct value; a linear function is used to express these values. Figure 4.18 shows the initial zero span circuit having only one variable resistor for both adjustments. This was improved later in the final zero span circuit to decouple the gain and offset effects in separate resistors.

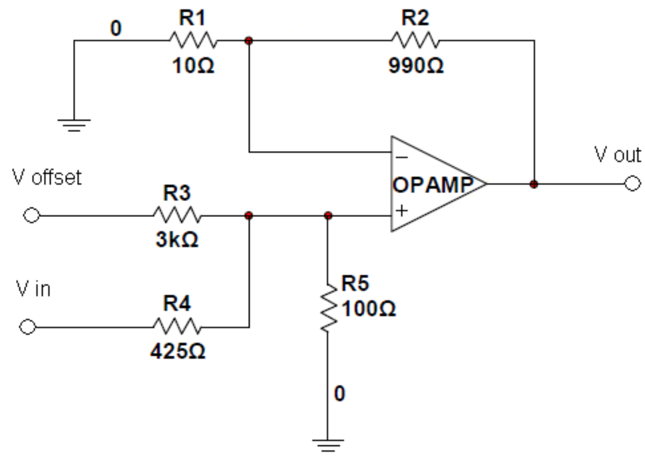

Figure 4.18 Initial zero span circuit.

The single phase conditioning circuit for testing purposes is shown in figure 4.19. Instrumentation amplifier, rectifier, and zero span stages are shown connected between them. This circuit was built as shown per phase to get the three phase system.

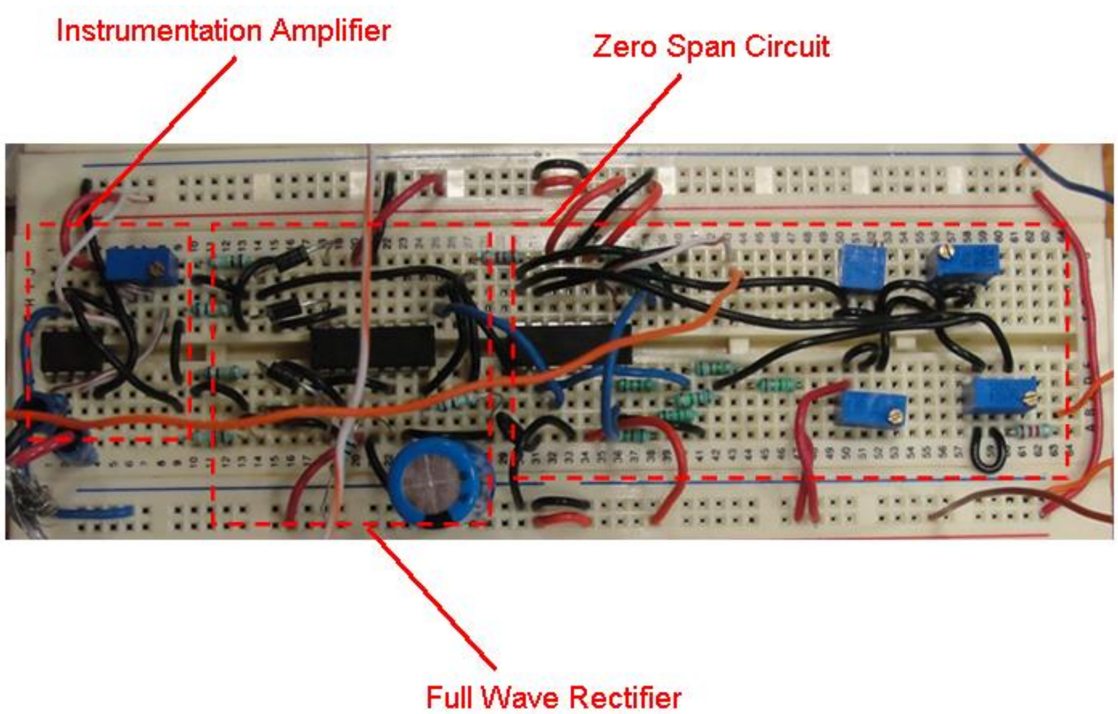

Figure 4.19 Single phase conditioning circuit over a breadboard.

4.4 Class 20 curve development

Values of multiple FLA and trip time were defined based on curve Class 20. Using an excel data sheet with a Power trend line option was defined this TIME equation function:

$$\text{TIME}= 1680*\text{FACTOR}\wedge (-2.7) +6 \qquad (3.6)$$

Figure 4.20 shows typical class 20 curve and TIME equation curve. There is less than 10 % error average between these curves; TIME equation was simulated to get the minimal impact in trip time, and focused when multiples of FLA was 5 or above, which are critical values due fast response needed. The TIME equation curve works only for over current trip condition. Table 4.5 shows the complete values for trip time compared between typical and TIME function.

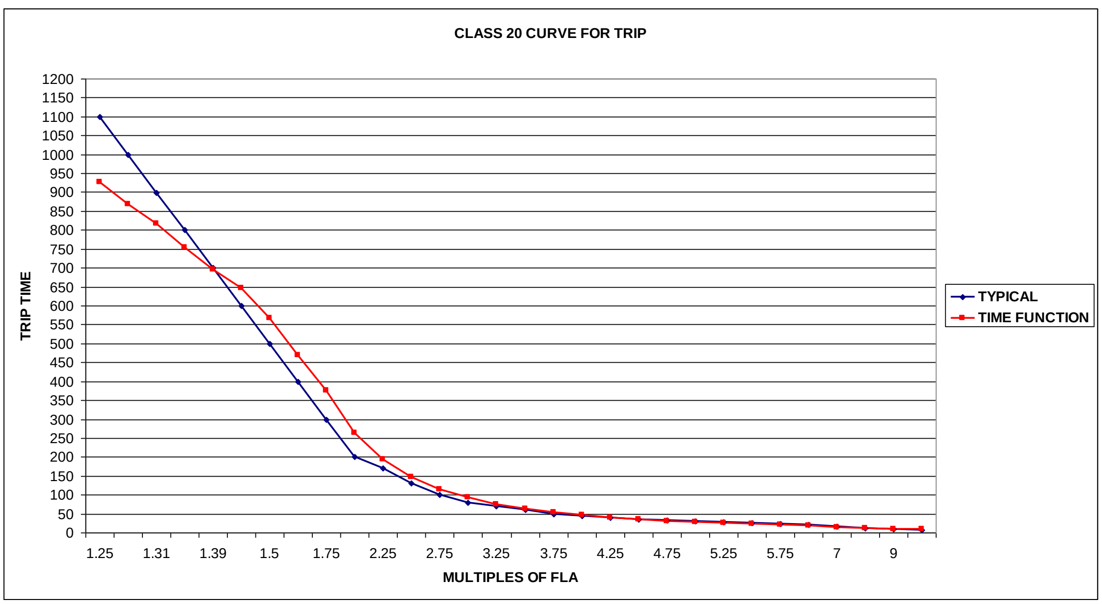

Figure 4.20 Typical class 20 curve and TIME equation curve.

Table 4.5 Typical Class 20 and TIME function trip time.

Multiples of FLA	FLA Amp.	Typical TRIP (sec)	TIME Function (sec)
1.25	56.25	1100	926
1.28	57.6	1000	869
1.31	58.95	900	816
1.35	60.75	800	753
1.39	62.55	700	697
1.43	64.35	600	646
1.5	67.5	500	568
1.61	72.45	400	470
1.75	78.75	300	377
2	90	200	265
2.25	101.25	170	194
2.5	112.5	130	148
2.75	123.75	100	115
3	135	80	93
3.25	146.25	70	76
3.5	157.5	60	63
3.75	168.75	50	53
4	180	45	46
4.25	191.25	40	40
4.5	202.5	35	35
4.75	213.75	33	31
5	225	30	28
5.25	236.25	28	25
5.5	247.5	25	23
5.75	258.75	23	21
6	270	20	19
7	315	16	15
8	360	12	12
9	405	9	10
10	450	7	9

4.5 Solid state overload relay test

This test was developed to verify the performance of actual solid state overload relay class 20. Overload relay was fed from 0 to 450 Amp with a three phase system in order to get trip time results. Overload relay was tested to get one of the three conditions of the trip: over current, unbalance and phase loss. Figure 4.21 shows only the over current trip condition test compared with the typical and TIME function. The overload relay trip time (marked in green), has values below the typical and TIME function specially when multiples of full load amps are below 5, which are not the critical. For multiples of full load amps above 5, the trip time is very similar to typical and TIME function, which these multiples are the critical. Even for multiples below 5, the solid state overload relay has values below typical and TIME function. The actual solid state overload relay works out of range specified for these values, but meet the overload protection purposes. Table 4.6 shows the complete values of the trip time compared with typical class 20 and TIME function.

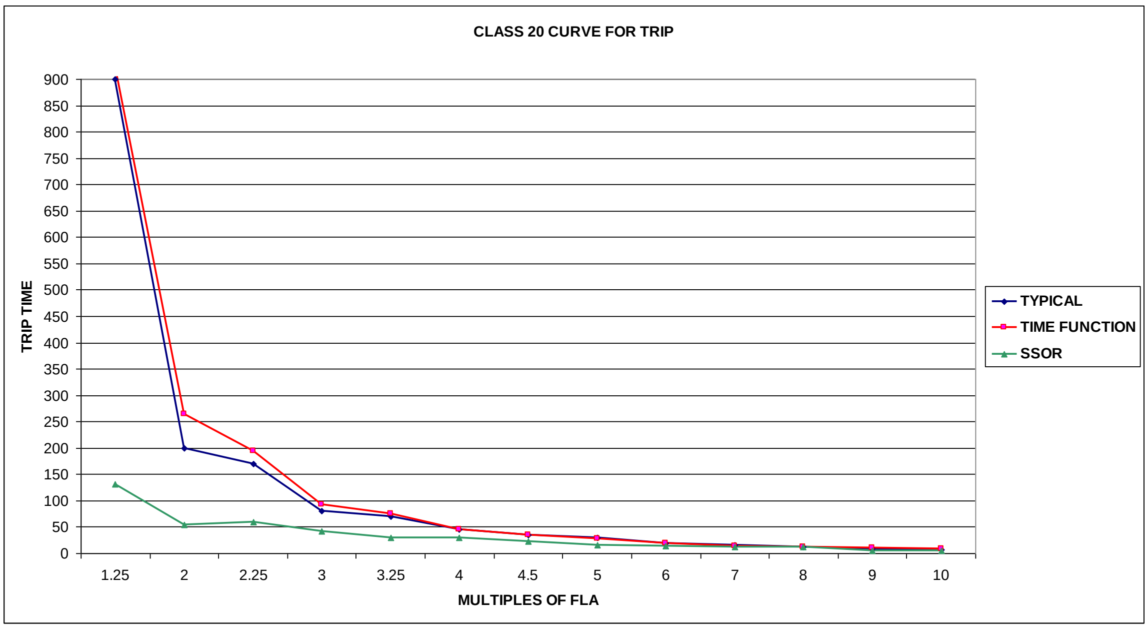

Figure 4.21 Solid state overload relay (SSOR) compared with Typical and TIME function for overcurrent condition.

Tables 4.7 and 4.8 show phase loss and unbalance test developed on the SSOR. As specification for both trip conditions, the relay should trip at 3 seconds when phase loss is present. The relay should trip when unbalance is above or below 25 % of nominal during 3 seconds. The over load relay works pretty close to this specification.

Table 4.6 SSOR trip time compared with Typical and TIME function for overcurrent condition.

Multiples of FLA	FLA Amp.	Typical TRIP (sec)	SSOR (sec)	TIME Function (sec)
1.25	56.25	900	132	926
2	90	200	54.0	265
2.25	101.25	170	60.0	194
3	135	80	42.0	93
3.25	146.25	70	29.4	76
4	180	45	28.9	46
4.5	202.5	35	23.0	35
5	225	30	16.6	28
6	270	20	13.6	19
7	315	16	12.0	15
8	360	12	12.7	12
9	405	9	5.6	10
10	450	7	5.3	9

Table 4.7 Phase loss solid state overload test.

Phase loss solid state overload test				
Phase	A	B	C	Trip time sec
Current AC	25	25	25	5
	20	20	20	2

Table 4.8 Unbalance solid state overload test.

Unbalance solid state overload test				
Phase	A	B	C	Trip time sec
Current AC	150	45	45	2
	100	45	45	3.8

4.6 Microprocessor test

This test was developed using the microprocessor already programmed with an external voltage source simulating the zero span 0-5 VDC signal. Figure 4.22 shows the microcontroller installed in the proto board wired to a LED device simulating the trip condition. With this test was verified the logical conditions, and measured the trip time. Table 4.9 shows these results. Some adjustments were developed to reduce the difference between microcontroller outputs and TIME function developed. Figure 4.23 shows comparison between microcontroller, solid state overload relay, typical and TIME function used on Eq. 3.6. Figure 4.23 shows only the over current trip condition test. The microprocessor trip time (marked in light blue), has a behavior very similar to TIME function which meets most of the multiples of full load amps.

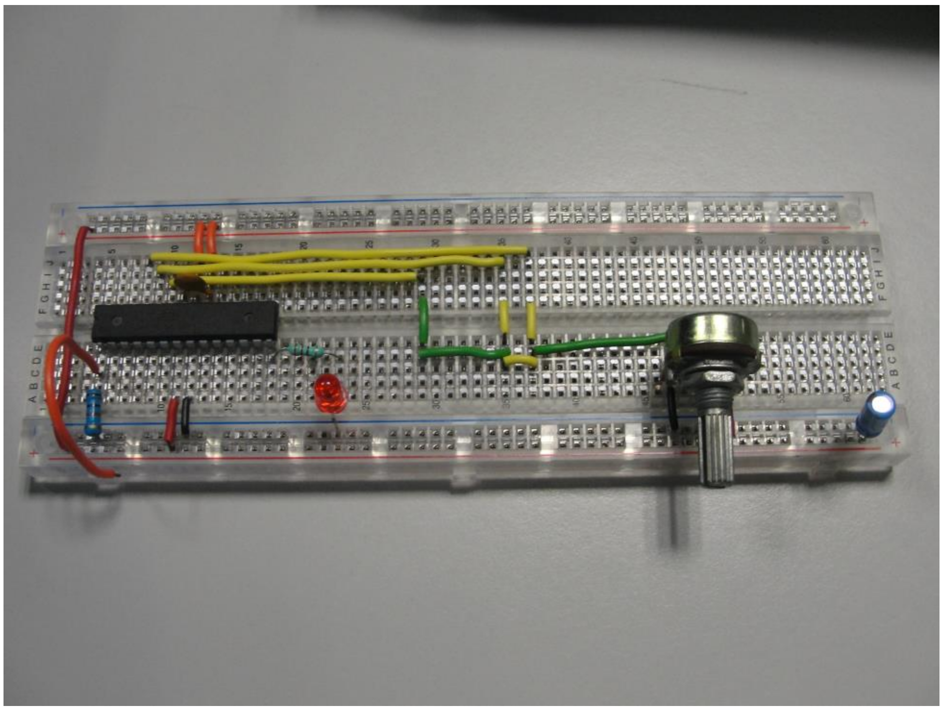

Figure 4.22 Microcontroller circuit test breadboard setup.

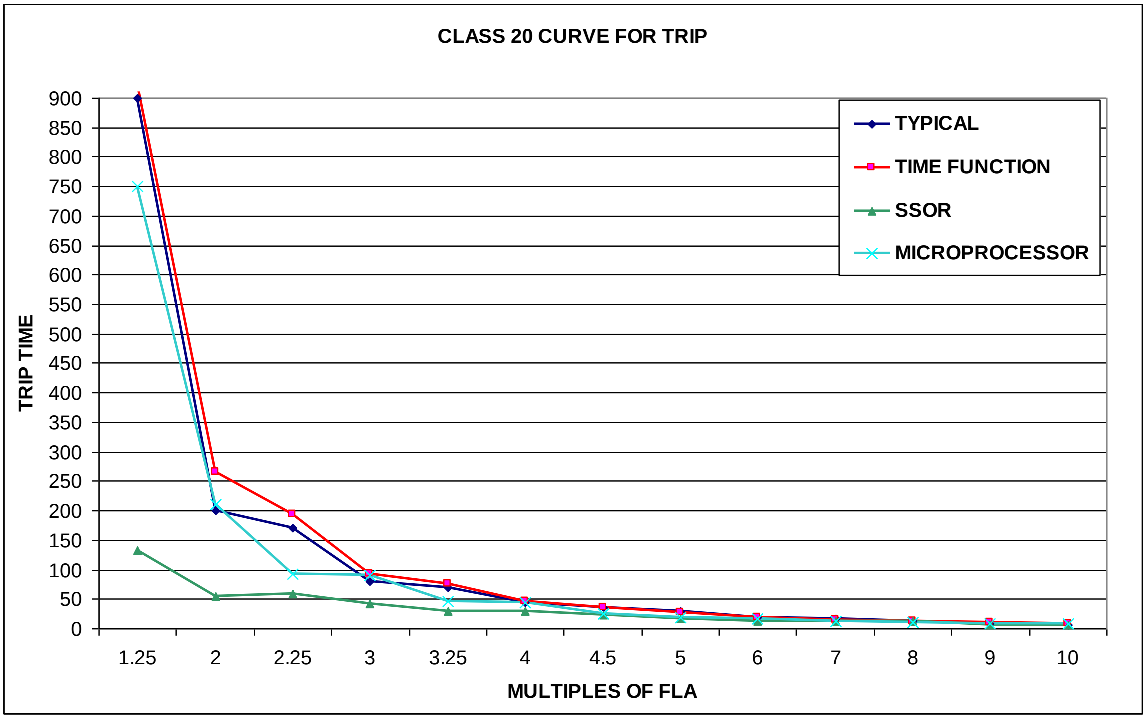

Figure 4.23 SSOR trip time test compared with Typical, TIME function and microprocessor for overcurrent conditions.

Table 4.9 SSOR trip time compared with Typical, TIME function and microprocessor for over current conditions.

Multiples of FLA	**FLA Amp.**	**Typical TRIP (sec)**	**SSOR (sec)**	**TIME Function (sec)**	**Microcontroller (sec)**
1.25	56.25	900	132	926	750
2	90	200	54.0	265	210
2.25	101.25	170	60.0	194	92
3	135	80	42.0	93	90
3.25	146.25	70	29.4	76	46
4	180	45	28.9	46	44
4.5	202.5	35	23.0	35	26
5	225	30	16.6	28	20
6	270	20	13.6	19	16
7	315	16	12.0	15	12
8	360	12	12.7	12	10
9	405	9	5.6	10	9
10	450	7	5.3	9	9

4.7 Actuator test circuit

The actuator circuit was verified to ensure voltage required to get energized the actuator coil. The figure 4.26 shows the actuator circuit that was developed using the voltage source, optocoupler and TIP device, and the original solid state overload actuator. A voltage source of 5 VDC was connected to the optocoupler terminals (+ and E) simulating the microcontroller output signal, another voltage source of 5VDC was connected to the optocoupler terminals (+ and D) having a TIP device as complement. With a voltage source of 5 VDC, the voltage needed to get energized the coil was about 3.2 VDC. Nominal voltage of coil calls for 3 VDC. Figure 4.8 shows the complete diagram. Figures 4.24 and 4.25 show the status of contacts 95-96, when the coil was de energized and energized due microprocessor signal.

When only the optocoupler was used, the actuator coil was not energized due to the lack of sufficient current from the opto-electronics device. The coil has very low impedance, about 6 ohms, and for their inductance, a TIP device was added in the circuit.

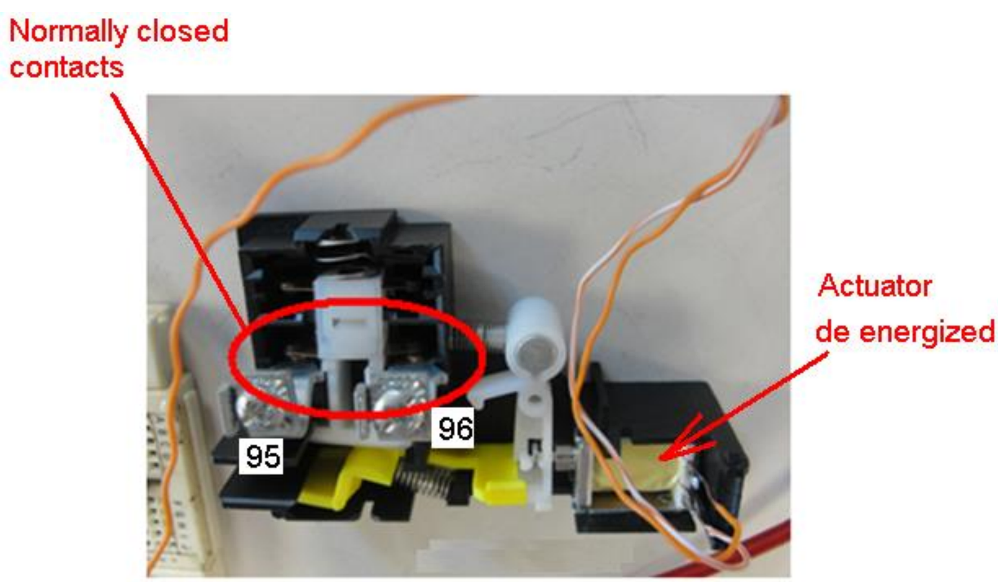

Figure 4.24 Actuator de energized. 95-96 overload relay contacts normally closed.

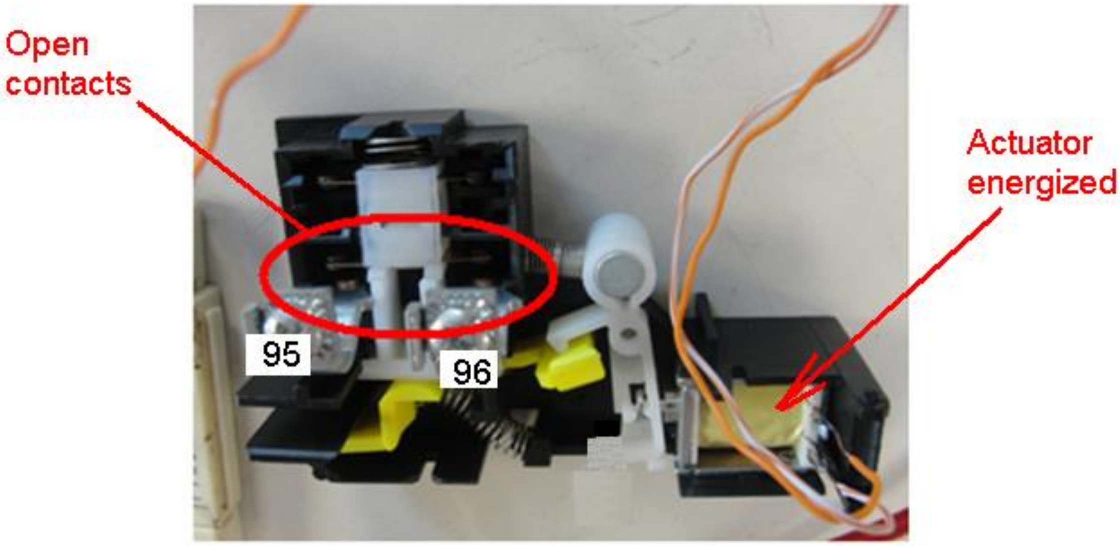

Figure 4.25 Actuator energized. 95-96 overload relay contacts normally open.

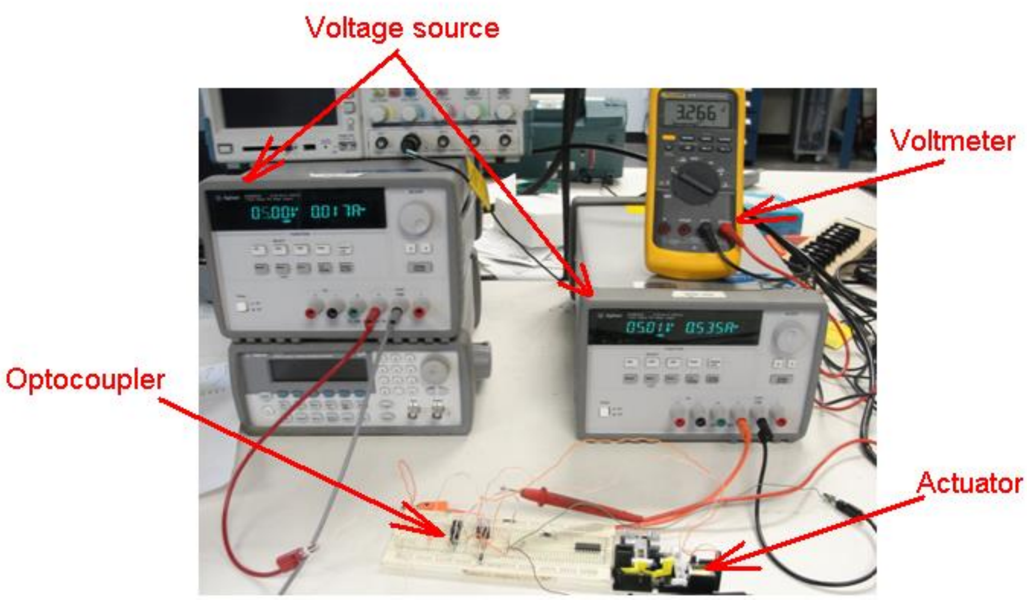

Figure 4.26 Actuator circuit test.

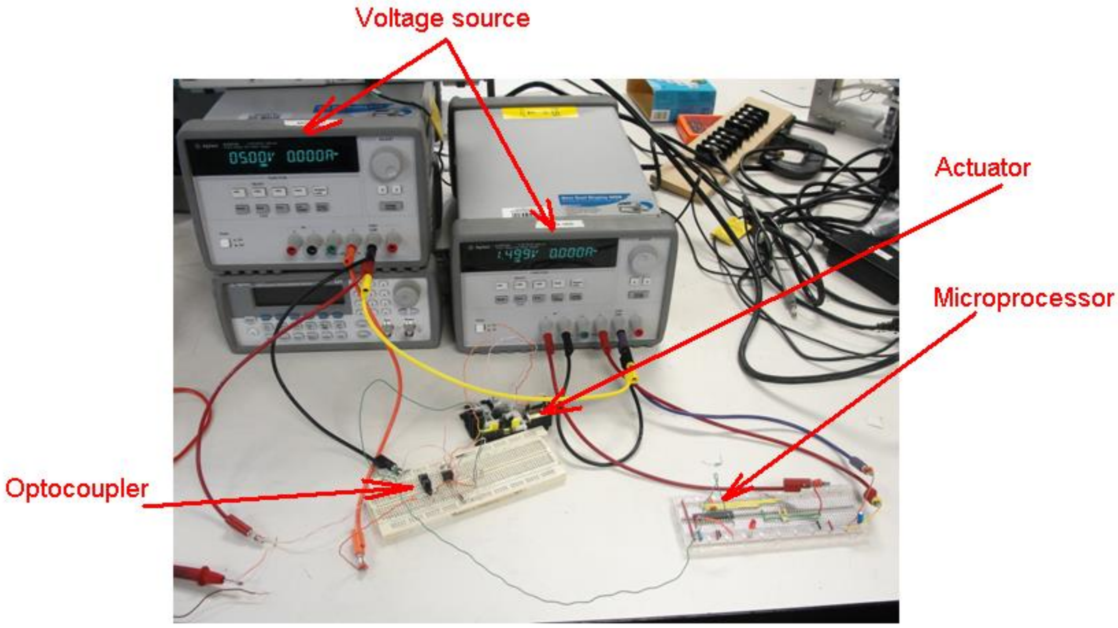

Figure 4.27 Actuator with microprocessor test.

Figure 4.27 shows a test connecting the actuator with the microprocessor device, in this test there were simulated the zero span VDC output voltages with an external source, based on trip condition program the coil actuator was energized. Table 4.9 shows these results.

4.8 Noise problems

Some of the problems found during conditioning signal and testing was a presence of some noise at the output of the sensor which once the instrumentation amplifier was connected this was eliminated. As was mentioned before, the variation in the output voltage signal amplified was improved when the instrumentation amplifier was changed to a single INA129P device. In addition, as some reference notes, the distance between the sensor and the electronic device to get amplified the signal is important due variations on the gain. Other important improvement is the use of proto board units, it was very common when a fail connection was made, and losses present due wiring length and device connections. It was used a Shield cable to get connected the sensor with the proto board unit to get eliminated the noise.

4.9 Integrated tests

Performance tests were developed using a three phase system current source. Three breadboard units with the same electronic devices were used to build the three phase sensor system. Figure 4.28 shows the three phase electronic signal conditioning circuits with their corresponding breadboard.

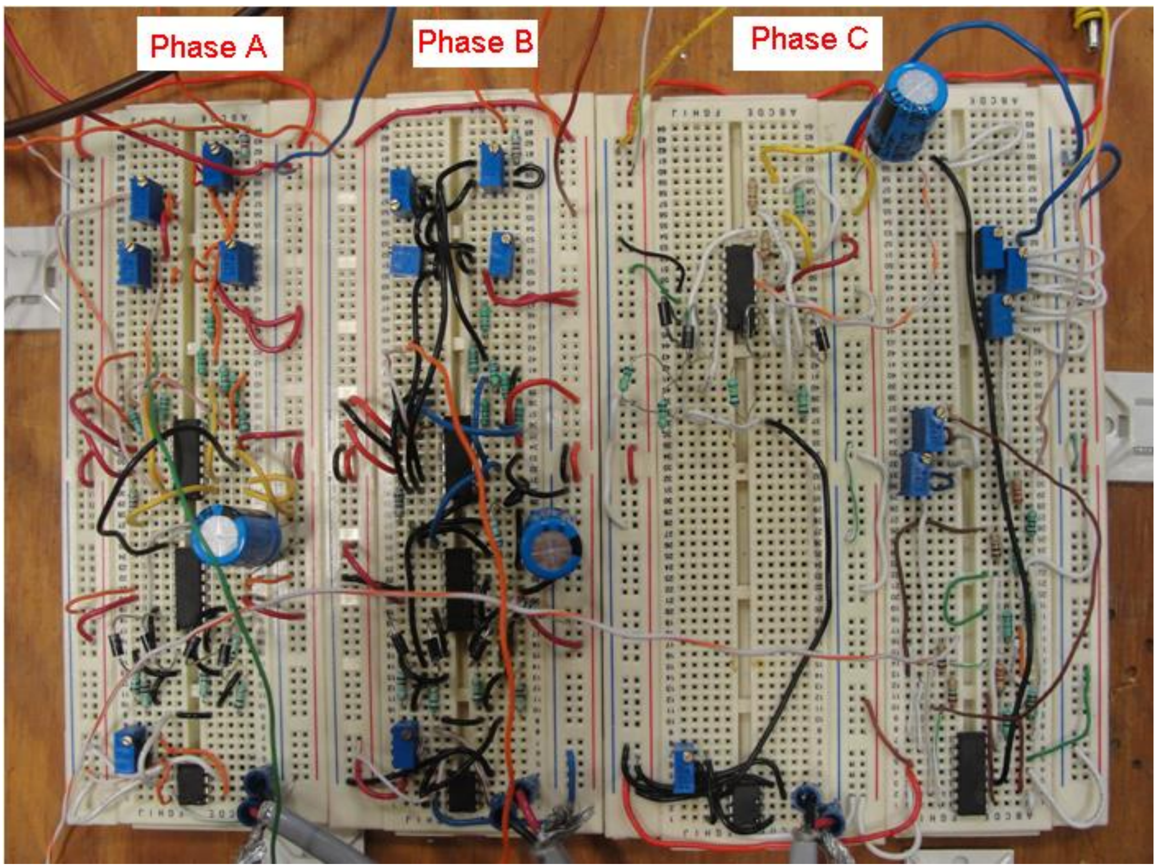

Figure 4.28 Three phase sensor test developed over breadboards.

Figure 4.29 shows a complete integrated test including the three phase sensor system, the conditioning signal per phase, actuator, optocoupler, microprocessor, voltage and current sources. Figure 4.30 shows a detail of the microprocessor wiring proto board used, it was added a reset button to get started a new test once a trip signal was present. Voltage regulator per phase were added to get microprocessor device protected in case of get an input from zero span stage circuit above 5 VDC.

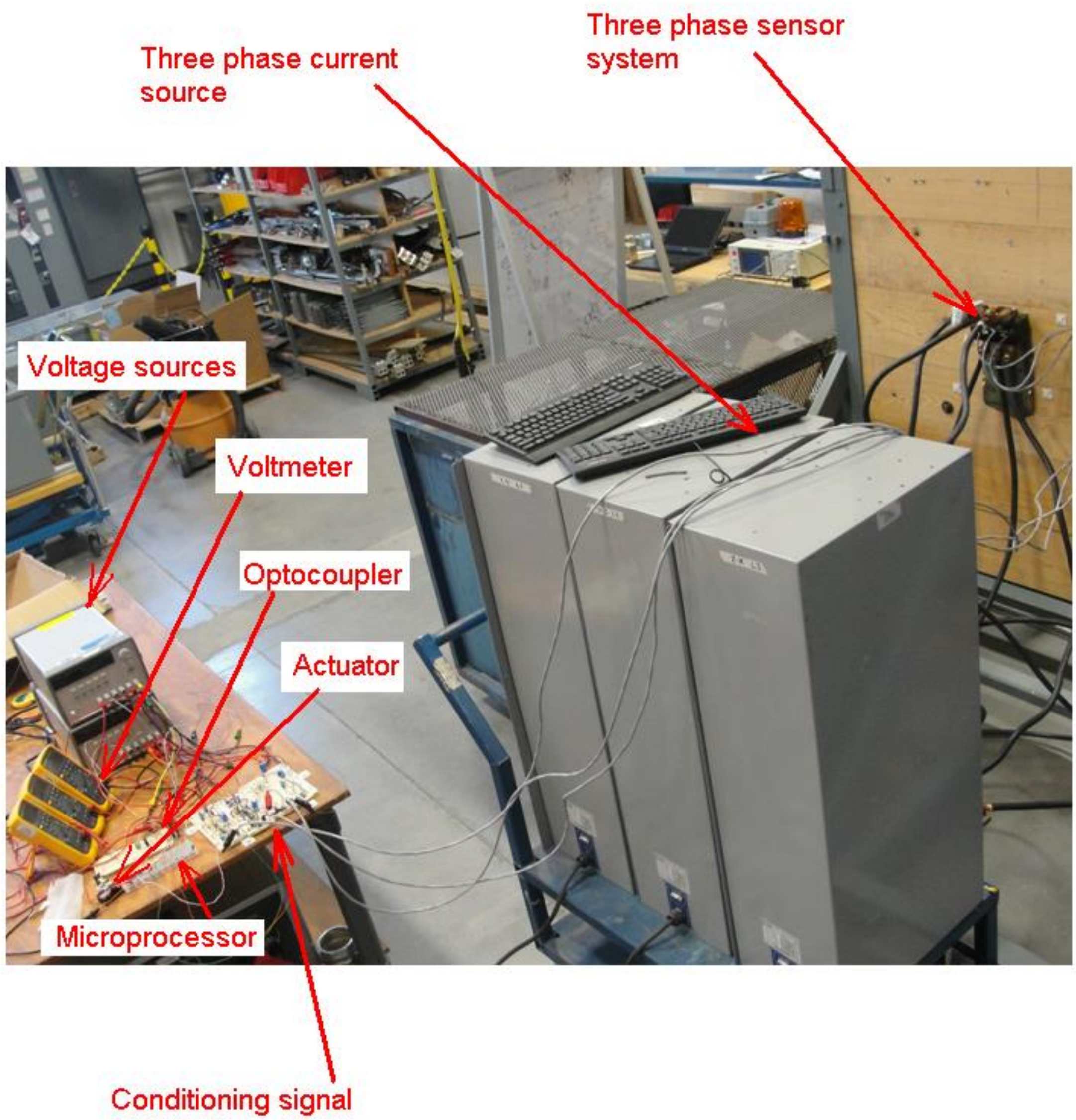

Figure 4.29 Complete integrated test for the three Phase RC-PCB SSOR device prototype.

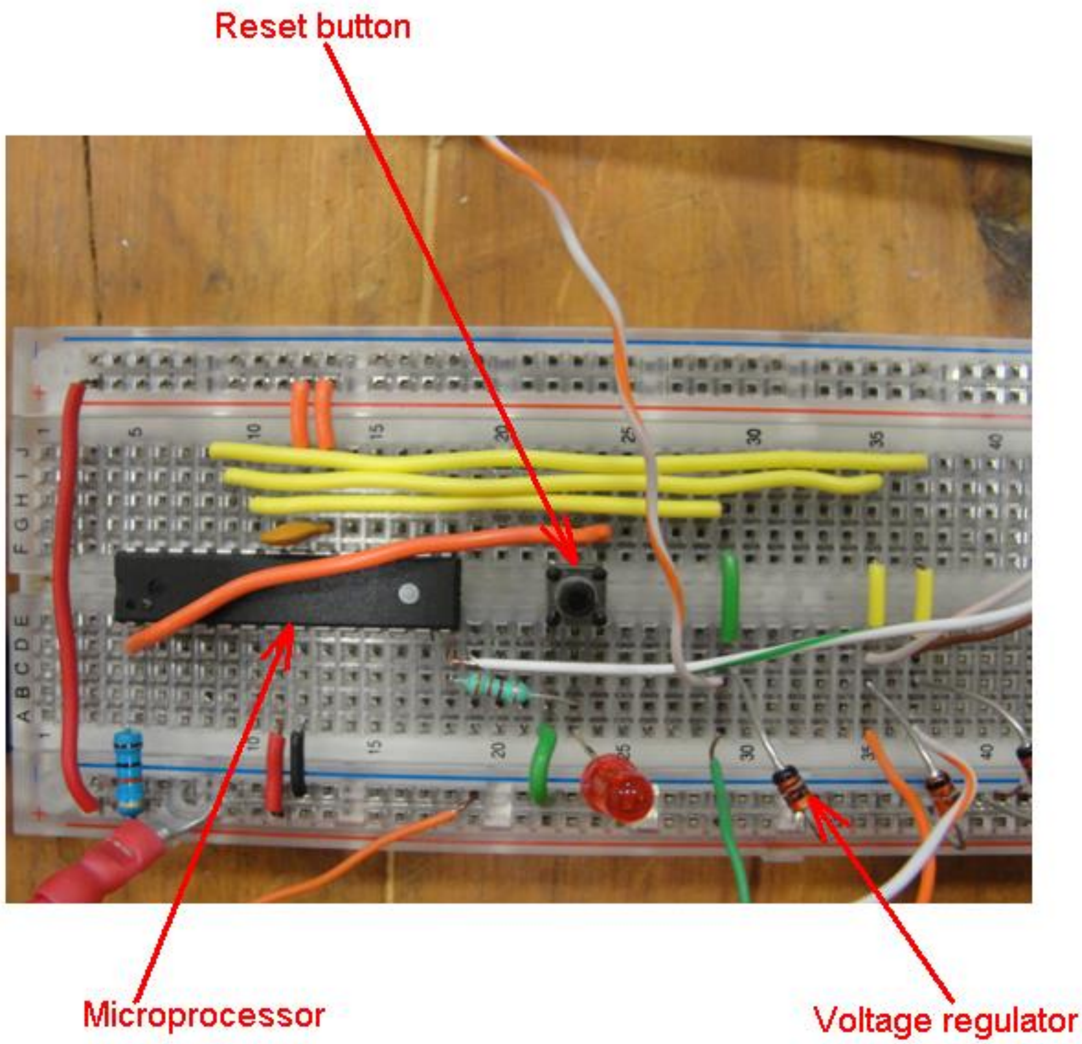

Figure 4.30 Microprocessor integrated test wiring detail.

Sensors were mounted in the actual CT carrier used on the solid state overload relay as figure 4.31 shows. Figure 4.32 shows the connection between each proto board with the DC source to get power for electronics. Figure 4.33 shows the connection between sensors and the three phase current source.

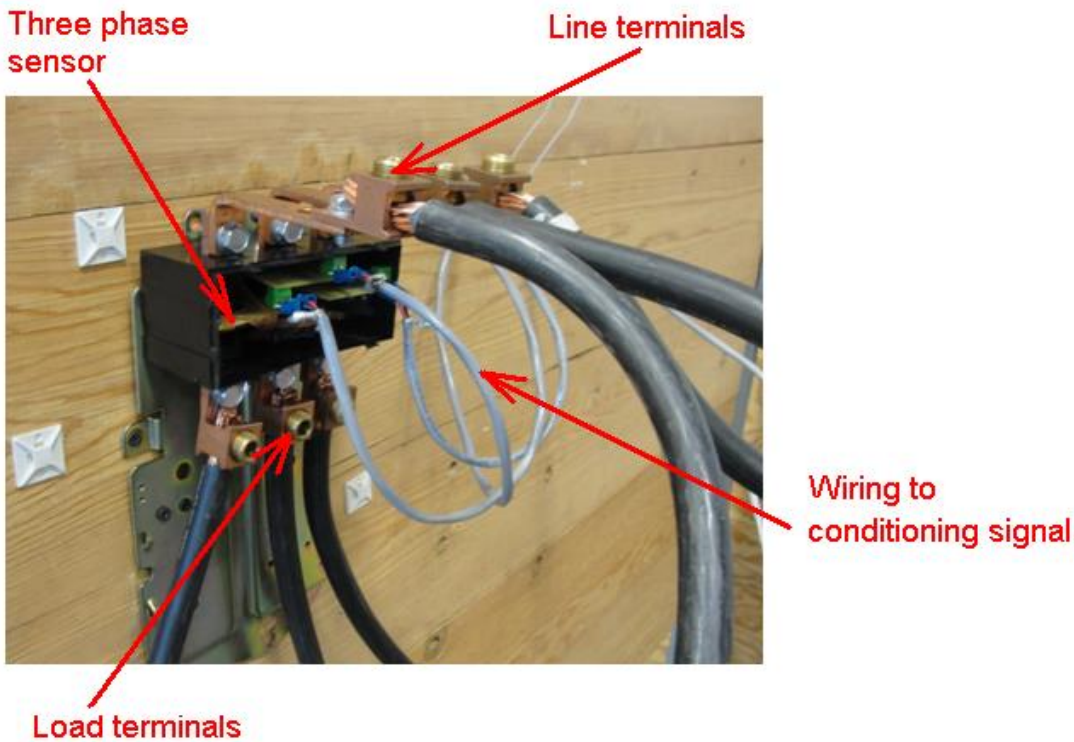

Figure 4.31 Three phase sensor mounted in carrier test developed.

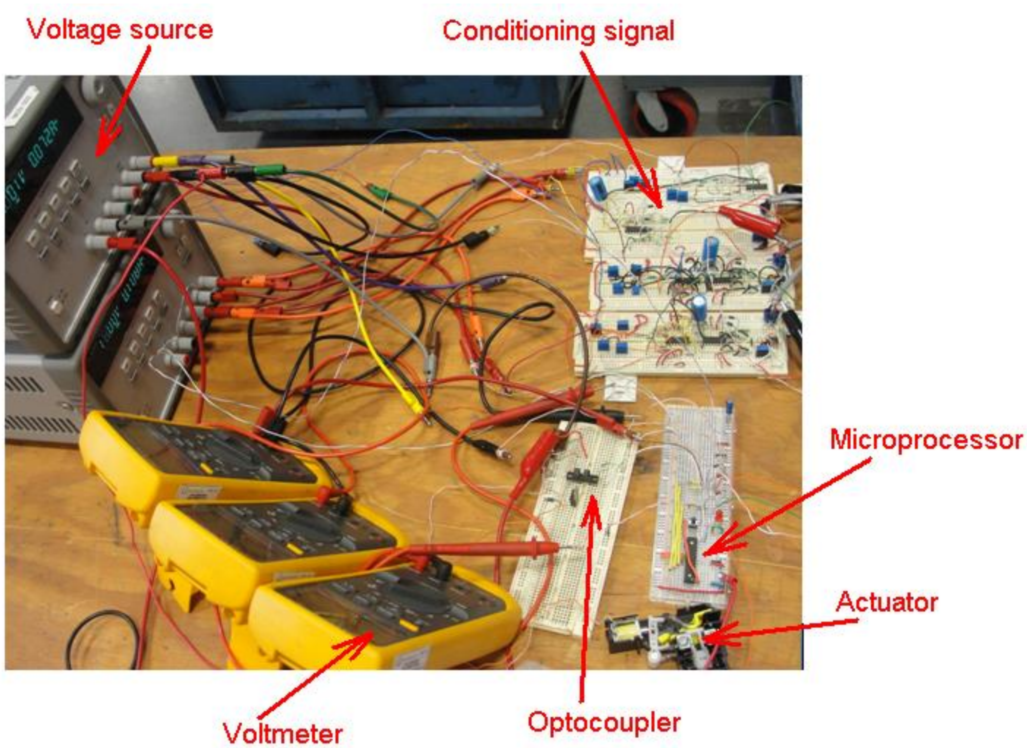

Figure 4.32 Three phase sensor test developed.

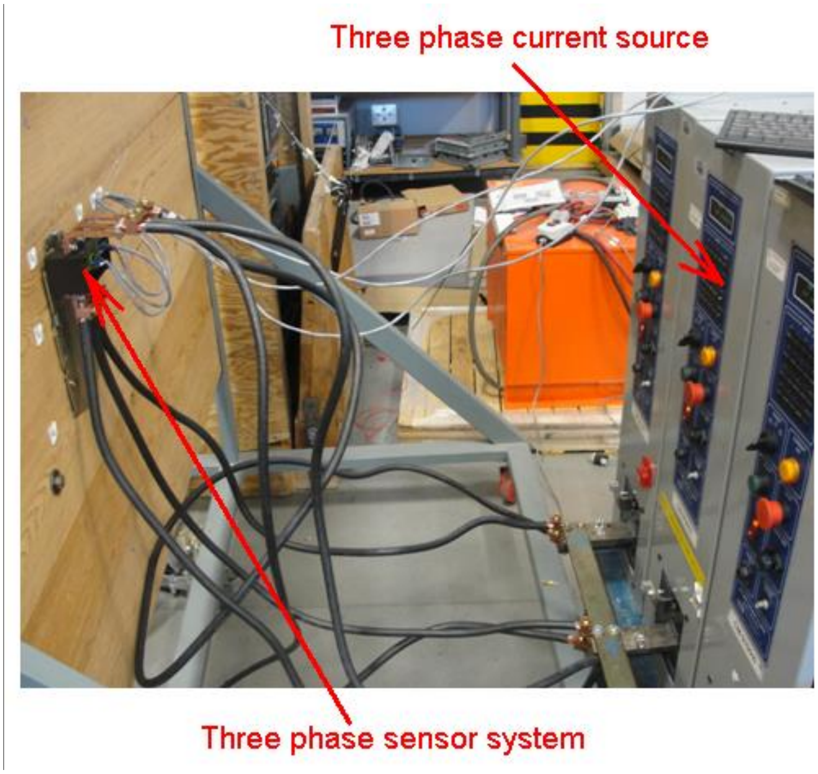

Figure 4.33 Three phase current source.

4.9.1 Test results

As the single phase test, in this case the gain was defined based on a precision, low power instrumentation amplifier device INA 129 which has a symmetrical array of three op-amp design. To setting the gain a variable resistor R_G was connected to the instrumentation amplifier as figure 4.9 shows. Output voltage from each sensor was connected to instrumentation amplifier to get V_{IN} signal according Figure 4.9. R_G for each phase was adjusted to get a gain value as table 4.10 shows, thus having an output voltage V_0 amplified for the next stage , for phase A, B and C.

Table 4.10: Instrumentation amplifier output for the three phase system.

Three phase Linearity test							
Current AC	Phase A mV	Phase B mV	Phase C mV	Output voltage sensor mV	Output Desired mV	Error	Gain
0	0	0	0	0	0	0.0	0
45	293	290	287	0.4	290	0.0	725
90	578	574	584	0.7	580	-0.2	827
135	870	860	880	1	870	0.0	870
180	1160	1150	1170	1.3	1160	0.0	892
225	1440	1440	1470	1.6	1450	0.0	906
270	1730	1720	1770	1.9	1740	0.0	916
315	1920	1920	1970	2.2	2030	-4.8	880
360	2230	2260	2300	2.5	2320	-2.5	905
405	2550	2580	2630	2.8	2610	-0.9	924
450	2600	2600	2700	3.1	2900	-10.1	849

Figure 4.34 shows the linearity test comparison between the three phases, there are some differences to get perfect linearity feature desired, about 10 % specially in high current values, suspected due current source doesn’t have the correct setting for some currents desired, and for electronics process; connection lost, length of cables, and potentiometer tolerances. This test was developed using the three phase system, passing a power cable throw each sensor and the cable connected to the three phase current source as figure 4.33 shows. An AC current range from 45 to 450 A. was injected to each circuit; the output voltage from each sensor was measured using an AC voltmeter. Table 4.10 shows the output voltage measured. Values of mV range were obtained, as expected.

Figure 4.34 Three phase system linearity test

4.9.2 Zero span I -V results

This test was developed using the three phase sensor system connected to the three phase current source. The conditioning signal per phase was connected to the sensors in order to get the zero span 0-5VDC. At 0 A. the output DC voltage required per phase should be 0 VDC, and for 450 A. the value expected per phase should be 5 VDC, which is the signal required for the microprocessor unit. Table 4.11 and figure 4.35 show those results. The zero span output signal per phase had a behavior expected. The zero span output signal for each AC current value had an average with an error less than 10% for currents above 90 A, and specially for those currents above 270 A, which are the critical with a trip time below 20 seconds. Even though the errors for currents of 45 and 90 A were 26.7% and 11% respectively, this is not a major concern due large trip time for overcurrent condition.

Table 4.11 Three phase zero span test results

Three phase zero span test						
Current AC	**Phase A VDC**	**Phase B VDC**	**Phase C VDC**	**Ideal VDC**	**Average VDC**	**Error %**
0	0	0	0	0	0.00	0.0
45	0.4	0.35	0.35	0.50	0.37	26.7
90	0.93	0.89	0.85	1.00	0.89	11.0
135	1.4	1.4	1.4	1.50	1.40	6.7
180	1.6	1.9	1.9	2.00	1.80	10.0
225	2.43	2.5	2.47	2.50	2.47	1.3
270	3.1	3.02	3.1	3.00	3.07	-2.5
315	3.5	3.3	3.4	3.50	3.40	2.8
360	3.8	3.99	4.1	4.00	3.96	0.9
405	4.4	4.4	4.3	4.50	4.37	3.0
450	5.05	5	4.92	5.00	4.99	0.2

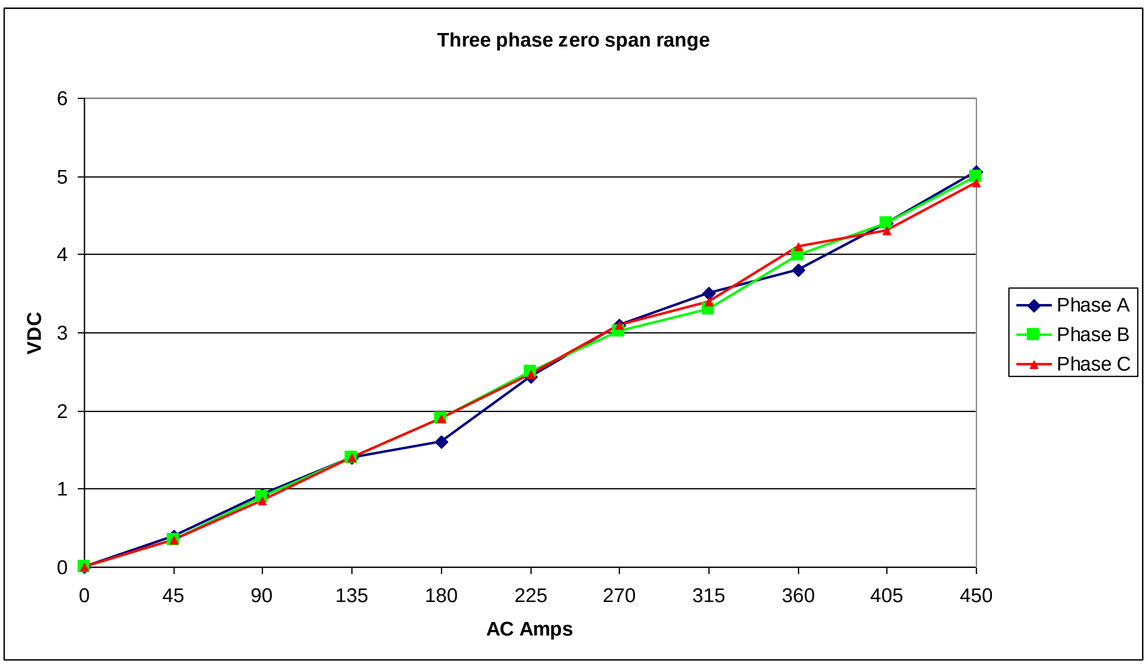

Figure 4.35 Three phase Zero span I-V test.

4.9.3 Three phase system with sensors and microprocessor

The three phase current source with a range from 0 to 450 A. was connected to the RC sensors, the output of each sensor was connected to their conditioning stage per phase. The 0-5 VDC output of the zero span conditioning signal per phase was connected to the microprocessor device inputs. The output of the microprocessor was connected to the actuator throw the optocoupler unit. This test was developed to verify the logical conditions and measure the trip time due overcurrent, unbalance and phase loss conditions using the complete system, including the three phase sensor system and the microprocessor device. An overcurrent condition was developed to measure the trip time to be compared with SSOR, typical, TIME function and microprocessor test. Table 4.12 shows these results and figure 4.36 illustrates them graphically. The sensor trip time due over current (marked in light blue), has a behavior very similar to the microprocessor test, as expected. The sensor curve has trip time values below TIME function due variations on the three phase zero span outputs, but for those which are critical, for high current values, the trip time is very similar to typical and TIME function. Table 4.13 and 4.14 show the phase loss and unbalance trip condition test, these tables show a comparison between SSOR trip time (which is sometimes below to 3 seconds), microprocessor test, and the complete test including sensor with microprocessor. For this comparison, the trip time condition was measured at 3 seconds for both conditions, which is the standard requirement for the SSOR.

Table 4.12 Overcurrent trip time three phase microprocessor test with sensor

Three phase microprocessor test										
Mutliples of FLA	**FLA Amp.**	**VDC**	**Phase A VDC**	**Phase B VDC**	**Phase C VDC**	**Sensor Trip time (sec)**	**Microcontroller (sec)**	**Typical TRIP (sec)**	**SSOR (sec)**	**TIME Function (sec)**
1.25	56.25	0.625	0.5	0.55	0.55	710	750	900	132	926
2	90	1.000	0.93	0.89	0.85	190	210	200	54.0	265
2.25	101.25	1.125	1.1	1.11	1,15	84	92	170	60.0	194
3	135	1.500	1.4	1.4	1.4	82	90	80	42.0	93
3.25	146.25	1.625	1.55	1.6	1.55	42	46	70	29.4	76
4	180	2.000	1.6	1.9	1.9	40	44	45	28.9	46
4.5	202.5	2.250	2.22	2.26	2.25	22	26	35	23.0	35
5	225	2.500	2.43	2.5	2.47	20	20	30	16.6	28
6	270	3.000	3.1	3.02	3.1	16	16	20	13.6	19
7	315	3.500	3.5	3.3	3.4	12	12	16	12.0	15
8	360	4.000	3.8	3.99	4.1	10	10	12	12.7	12
9	405	4.500	4.4	4.4	4.3	9	9	9	5.6	10
10	450	5.000	5.05	5	4.92	8	9	7	5.3	9

Table 4.13 phase loss trip condition test

Phase loss trip condition test						
Phase	**A**	**B**	**C**	**SSOR Trip time (sec)**	**Micro test**	**Sensor/ microprocessor**
Current AC	25	25	25	5	3	3
	20	20	20	2	3	3

Table 4.14 Unbalance trip condition test

Unbalance trip condition test						
Phase	**A**	**B**	**C**	**SSOR Trip time (sec)**	**Micro test**	**Sensor/ microprocessor**
Current AC	150	45	45	2	3	3
	100	45	45	3.8	3	3

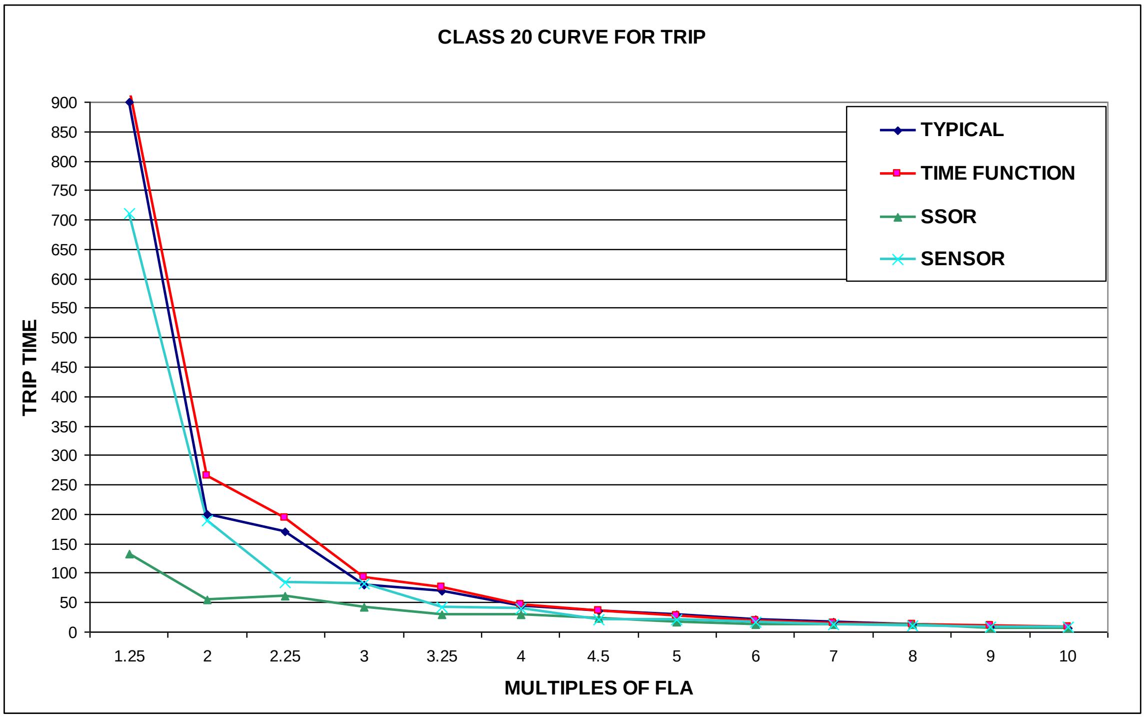

Figure 4.36 SSOR trip time test compared with Typical, TIME function and PCB sensor for over current conditions.

Chapter 5: Conclusions

The main objective of this research was to develop a device which can be used as an overload relay using a RC sensor instead of the conventional CT based on the solid state overload relay condition trip. This requirement was reached for overcurrent, unbalance and phase loss trip conditions.

Based on the Typical trip curve for class 20, and overcurrent condition, the difference on trip time is higher in SSOR than RC sensor compared with Typical trip curve specially for current values below 180 A. Time difference is about 110 to 750 seconds and 90 to 190 seconds for the SSOR and RC sensors, respectively. Even for critical values, where the current is high, above 270 A, the trip time difference is higher on SSOR. The RC sensor has a better performance than SSOR according to the typical trip curve class 20 requirement. The SSOR works below the typical function, and the RC works pretty close to this curve. For unbalance and phase loss trip conditions, the RC sensor has trip time values equal to specification required to 3 seconds, compared with SSOR which has vales only closer to this request. Based on these results obtained, the RC sensor can be taken as a replacement of the standard CT used in the solid state overload relay to get the trip condition required.

Output signals to get a trip were successfully obtained regardless of losses due distance between sensor and electronic stage, the usage of a proto board prototype, rectification process, current losses, and variable potentiometer tolerances. Additional opportunity areas to reduce losses are reviewed for future research to get an improvement in the sensor performance.

A very extensive application of the RC sensors can be developed specially by their excellent linear response without saturation problems, for this research it was developed up to 450 A without this problem and showing a difference in most of the current values below of 10 %. With this special feature, in addition with the RC sensor as a replacement of the CT, and the low cost and size reduced impact; the improvement of the actual SSOR has an important opportunity area to be developed, and not only for one specific range of currents.

Chapter 6: Future Research

Further research is needed to address some concerns, device potential and possibilities of the RC sensors. The following project possibilities and details are recommended:

1. To Review option to get adjustment for several ranges of amperes in the same sensor.
2. To improve the power supply used for electronics devices.
3. To improve the housing to allocate electronic device with sensors according dimensions and specifications required.
4. To improve the size of the conditioning signal using a multiplexer device in order to reduce from three to one conditioning signal circuit.
5. To improve the noise and adjustment variations by developing an electronic conditioning stage printed.
6. To evaluate physical changes to this product, parts and assembly's necessary as well as the tests required according standard norms defined to get certified the product. This includes the PCB sensor printed with all conditioning signal using Gerber files. Figure 6.1 shows a model proposal for the installation of the PCB sensors in the actual CT carrier used in solid state over load relay. The three phase PCB sensors are mounted in this carrier modified with a kind of clip to get the sensors fixed to the carrier.

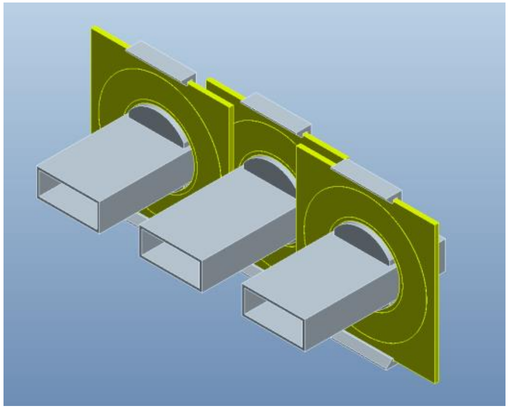

Figure 6.1 Proposed model of PCB sensor carrier.

Appendix

I Datasheets

INA129
http://www.ti.com/lit/ds/sbos051b/sbos051b.pdf

LM324
http://pdf1.alldatasheet.com/datasheet-pdf/view/22753/STMICROELECTRONICS/LM324.html

TL084
http://www.datasheetcatalog.org/datasheet/stmicroelectronics/2301.pdf

IN4004
http://pdf1.alldatasheet.com/datasheet-pdf/view/329384/CHENG-YI/IN4004.html

ATMEGA168
http://pdf1.alldatasheet.com/datasheet-pdf/view/313544/ATMEL/ATmega168.html

TIP 41
http://pdf1.alldatasheet.com/datasheet-pdf/view/2782/MOSPEC/TIP41.html

II Morphology analysis

		Detection	Protection	Measure	Control/Monitoring
Device factor "where is used"	Overload relay		●●		●
	Busway			●	
	Power panel				
	Breaker				
	Load center				
	Motor Control Center				
	Motor failures	●●●	●●●	●	
	Motor starters		●●●		●
	Power transformers			●	
	General application		●●●● ●●●	●●● ●●● ● ●●● ●●	●●● ●●

III Microprocessor codes

```
/*
 * Code.c
 * Project:              Overcurrent Monitor
 * Created:              March 2013
 * Version:              0.1
 * Author :              Vicente Noguez
 * Company:              Schneider Electric
 *
 * Chip type      :      ATmega168P
 * Clock frequency:      8.00 MHz = 125 ns per operation
 *
 * Operating conditions
 * ADC resolution  :     10 bits
 * Input data range:     0 to 450A = 0 to 5Vdc = 0d0000 to 0d1024
 * Nominal current :     FLA = 45A = 0.5Vdc = 0d0102
 * Overcurrent time:     depends of the factor
 * Unbalance time  :     3s
 * Phase loss time :     3s
 */


/* Definition of constants: ADC register, CPU frequency */
#define ADC_PHASE_A      0x40
#define F_CPU            8000000UL
#define EXPNT            2.7
//#define FACTD          102                         //45 * a factor to convert
bits to current
#define K                55646744064
//210,000*(45*bits_to_current=102)^2.7
#define failure_signal  PORTB |= _BV(0)

#include <avr/io.h>
#include <util/delay.h>
#include <avr/interrupt.h>
#include <stdio.h>
#include <math.h>


/* Declaration of global variables */
char fovc, funb, fphl;
int  tunb, tphl;
long tovc;
long time;               //Time treshold


/* TIMER0 interrupt routine: it is called when TIMER0 overflows */
ISR(TIMER0_OVF_vect) {
       TCNT0  = 0x06;
       tovc++;
}

/* TIMER1 interrupt routine: it is called when TIMER1 overflows */
```

```
ISR(TIMER1_OVF_vect) {
        TCNT1   = 0xFF06;
        tunb++;
}

/* TIMER2 interrupt routine: it is called when TIMER2 overflows */
ISR(TIMER2_OVF_vect) {
        TCNT2   = 0x06;
        tphl++;
}


/*** SUPPORT FUNCTIONS. They help to make calculations in the core functions
***/

/* Find the maximum of three values */
int findMax(int a, int b, int c){
    int max = a;
    if(max < b)
        max = b;
    if(max < c)
        max = c;
    return max;
}

/* Calculate the absolute value */
int absval(int x){
    if (x < 0)
        x = -x;
    return x;
}

/* Calculate the time current factor */
long findTime(int max){
    long timex;
    timex = (long)(K/pow(max,EXPNT)+625);
    return timex;
}

/* Set and reset timers */
void set_ovc(){
    TCCR0B = 0x04;
    TCNT0  = 0x06;
    tovc   = 0;
    fovc   = 1;
}

void set_unb(){
    TCCR1B = 0x04;
    TCNT1  = 0xFF06;
    tunb   = 0;
    funb   = 1;
}

void set_phl(){
    TCCR2B = 0x06;
    TCNT2  = 0x06;
    tphl   = 0;
    fphl   = 1;
}
```

```
void clr_ovc(){
    TCCR0B = 0x00;
    TCNT0  = 0x06;
    tovc   = 0;
    fovc   = 0;
}

void clr_unb(){
    TCCR1B = 0x00;
    TCNT1  = 0xFF06;
    tunb   = 0;
    funb   = 0;
}

void clr_phl(){
    TCCR2B = 0x00;
    TCNT2  = 0x06;
    tphl   = 0;
    fphl   = 0;
}

/*** CORE FUNCTIONS. They determine overcurrent, unbalance or phase loss
conditions ***/

/* Overcurrent routine*/
void findOvercurrent(int a, int b, int c){
    //int pdif;
    int pmax;
    pmax = findMax(a,b,c);
    //1.25 FLA = 0d0128
    if(pmax >= 128){
        time = findTime(pmax);
        if(!fovc){
            set_ovc();
        }
    } else {
        clr_ovc();
    }
}

/* Unbalance routine */
void findUnbalance(int a, int b, int c){
    int avg, deva, devb, devc, dmax, unb;
    avg  = (a+b+c)/3;
    deva = absval(a-avg);
    devb = absval(b-avg);
    devc = absval(c-avg);
    dmax = findMax(deva,devb,devc);
    unb  = (100*dmax)/avg - 25;
    //Start timer if value is 25% above
    if(unb >= 0){
        if(!funb){
            set_unb();
        }
    //If value is not 25% above and trigger is set, then clear
    } else {
        clr_unb();
    }
}

/* Phase loss routine */
```

```
void findPhaseLoss(int a, int b, int c){
    int avg;
    avg = (a+b+c)/3;
    //If A=0, B=0, C=0, or AV<25% of 0.5Vdc (0d25), start timer
    if ((a < 10 || b < 10) || (c < 10 || avg < 25)){
        if(!fphl){
            set_phl();
        }
    } else {
        clr_phl();
    }

}


/*** INITIALIZATION FUNCTIONS. Assign initial values to registers ***/

/* Initialize timers */
void set_timer(char timer, char set_tccrXb, char set_timskX, short set_tcntX){
    if (timer == 0){
       TCCR0B = set_tccrXb;             //It will be enabled with TCCR0B =
0x04;
       TIMSK0 = set_timskX;
       TCNT0  = set_tcntX;
    } else if (timer == 1) {
       TCCR1B = set_tccrXb;             //It will be enabled with TCCR1B =
0x04;
       TIMSK1 = set_timskX;
       TCNT1  = set_tcntX;
    } else {
       TCCR2B = set_tccrXb;             //It will be enabled with TCCR2B =
0x04;
       TIMSK2 = set_timskX;
       TCNT2  = set_tcntX;
    }
}



/*** MAIN FUNCTION ***/
int main(void) {

       /*Definition and initialization of variables */
       int a, b, c = 0;
       char phase  = 0;
       char  rflag = 0;
       time        = 0xFFFFFFFF;
       fovc        = 0;
       funb        = 0;
       fphl        = 0;
       tovc        = 0;
       tunb        = 0;
       tphl        = 0;

       /* ADC setup: analog comparator disabled, ADC enabled, ADC0 as input */
       ACSR   = 0x80;                //Analog comparator disabled
       ADCSRA = 0x87;                //ADC enabled, conversion not yet started
(ADCSRA = (1<<ADEN)), clk/128
       ADCSRB = 0x00;                //Free running mode
       ADMUX  = ADC_PHASE_A;         //Start conversion with data from phase A
```

```
	/* Timers setup: /256 prescaling (31.25kHz), enable timer overflow
interrupts,
	 * count starts from -250 to have time frames of 8ms (250*32us) */
	set_timer(0,0x00,0x01,0x06);
	set_timer(1,0x00,0x01,0xFF06);
	set_timer(2,0x00,0x01,0x06);

	/* Ports setup: PB has the trigger output, PC has the analog inputs is
the analog sensor */
	DDRB  = 0xFF;
	DDRC  = 0x00;
	PORTB = 0x00;

	/* Enable Interrupts */
	sei();

	while (1){

		/* Read value from ADC */
		ADCSRA |= (1<<ADSC);		//Start ADC conversion
		while (ADCSRA & (1<<ADSC));	//Wait until conversion is
complete

		if(phase == 0){
		    a = ADCW;
		    phase++;
		    ADMUX++;
		} else if (phase == 1) {
		    b = ADCW;
		    phase++;
		    ADMUX++;
		} else {
		    c = ADCW;
		    phase = 0;
		    ADMUX = ADC_PHASE_A;
		    rflag = 1;
		}

		/*rflag indicates when at least one value of each phase was read
to avoid nuissance tripping*/
		if(rflag){

		    rflag = 0;

		    findOvercurrent(a,b,c);
		    findUnbalance(a,b,c);
		    findPhaseLoss(a,b,c);

		    if(tovc >= time){
		        failure_signal;
		    } else if(tunb >= 375 || tphl >= 375){
		        failure_signal;
		    }

		    _delay_ms(500);

		}



	}
```

```
return 1;
```

References

[1] Zhang, X. H., Y. N. Cao, et al. (2001). A new project for motor fault detection and protection. Developments in Power System Protection, 2001, Seventh International Conference on (IEE).

[2] Alwin, P. E. (1995). Advanced motor protection and communications with solid state motor protective devices. Cement Industry Technical Conference, 1995. XXXVII Conference Record., 1995 IEEE.

[3] Kojovic, L. A. (2008). Advanced Protective Relaying Based on Rogowski Coil Current Sensors. Developments in Power System Protection, 2008. DPSP 2008. IET 9th International Conference on.

[4] Kojovic, L. J. A. (2006). Application of Rogowski Coils used for Protective Relaying Purposes. Power Systems Conference and Exposition, 2006. PSCE '06. 2006 IEEE PES.

[5] Kojovic, L. A. (2005). Applications of Rogowski coils for advanced power system solutions. Electricity Distribution, 2005. CIRED 2005. 18th International Conference and Exhibition on.

[6] Kojovic, L. A. (2007). Comparative Performance Characteristics of Current Transformers and Rogowski Coils used for Protective Relaying Purposes. Power Engineering Society General Meeting, 2007. IEEE.

[7] Poncelas, O., J. A. Rosero, et al. (2008). Design and application of Rogowski coil current sensor without integrator for fault detection in induction motors. Industrial Electronics, 2008. ISIE 2008. IEEE International Symposium on.

[8] Hewson, C. and W. R. Ray (2004). The effect of electrostatic screening of Rogowski coils designed for wide-bandwidth current measurement in power electronic applications. Power Electronics Specialists Conference, 2004. PESC 04. 2004 IEEE 35th Annual.

[9] Kang-Won, L., P. Jeong-Nam, et al. (2001). Geometrical effects in the current measurement by Rogowski sensor. Electrical Insulating Materials, 2001. (ISEIM 2001). Proceedings of 2001 International Symposium on.

[10] Kelly, J. P. (1990). IEC and NEMA motor starters: understanding the differences. Textile, Fiber and Film Industry Technical Conference, 1990., IEEE 1990 Annual.

[11] Poncelas, O., J. A. Rosero, et al. (2009). "Motor Fault Detection Using a Rogowski Sensor Without an Integrator." Industrial Electronics, IEEE Transactions on 56(10): 4062-4070.

[12] Gary, W. and G. R. Taylor (1975). "New Concept in Motor and Motor Circuit Protection." Industry Applications, IEEE Transactions on IA-11(5): 564-570.

[13] Schatz, M. W. (1971). "Overload Protection of Motors---Four Common Questions." Industry and General Applications, IEEE Transactions on IGA-7(2): 196-207.

[14] Kojovic, L. A. (2003). PCB Rogowski coil designs and performances for novel protective relaying. Power Engineering Society General Meeting, 2003, IEEE.

[15] Kojovic, L. (2002). "PCB Rogowski coils benefit relay protection." Computer Applications in Power, IEEE 15(3): 50-53.

[16] Kojovic, L. (1997). "Rogowski coils suit relay protection and measurement [of power systems]." Computer Applications in Power, IEEE 10(3): 47-52.

[17] Dupraz, J. P., A. Fanget, et al. (2007). Rogowski Coil: Exceptional Current Measurement Tool For Almost Any Application. Power Engineering Society General Meeting, 2007. IEEE.

[18] Abdi-Jalebi, E. and R. McMahon (2005). Simple and Practical Construction of High-Performance, Low-Cost Rogowski Transducers and Accompanying Circuitry for Research Applications. Instrumentation and Measurement Technology Conference, 2005. IMTC 2005. Proceedings of the IEEE.

[19] Garza, G. (2011) .Current Sensors development using PCB Rogowski coil technology. ITESM, Thesis investigation M.C. degree.

[20] Kojovic, L. A. (2003). Split-core PCB Rogowski coil designs and applications for protective relaying. Transmission and Distribution Conference and Exposition, 2003 IEEE PES.

[21] Franco, S. (1998). ”Design with Operational Amplifiers and Analog Integrated Circuits.” WCB McGraw-Hill. Second Edition.

[22] Fisher, L. E. (1966). "Transient Thermal Performance of Busways at High Values of Overload Current for Short Periods of Time." Industry and General Applications, IEEE Transactions on IGA-2(6): 480-484.

[23] Ward, D. A. and J. L. T. Exon (1993). "Using Rogowski coils for transient current measurements." Engineering Science and Education Journal 2(3): 105-113.

[24] Brighton, R. J. and P. N. Ranade (1982). "Why Overload Relays Do NOT Always Protect Motors." Industry Applications, IEEE Transactions on IA-18(6): 691-697.

[25] Overload Relays and Thermal Unit Selection Class 9065, Schneider Electric, 1998.

[26] US patent 5414400. Jean Paul Gris, Jean Pierre Dupraz, " Rogowski Coil ", 1995-05-09.

[27] US patent 5442280. Christophe Baudart." Device measuring an electrical current in a conductor using a Rogowski coil", 1995-08-15.

[28] US patent 6313623. Ljubomir A. Kojovic, Veselin Skendzic, Stephen E. Williams, Franklin, "High precision Rogowski coil", 2001-11-06.

[29] Altium software. www.altium.com

[30] Multisim software. www.ni.com